공 학 박 사 학 위 논 문

Electrochemical System for Selective Removal of Phosphate

선택적 인산제거를 위한 전기화학 시스템

2020년 2월

서울대학교 대학원

화학생물공학부

홍 성 필

Electrochemical System for Selective Removal of Phosphate

by

Sung Pil Hong

under the supervision of

Professor Changha Lee, Ph. D.

A dissertation submitted in partial fulfillment of the requirements for the Degree of

Doctor of Philosophy

February 2020

SCHOOL OF CHEMICAL AND BIOLOGICAL ENGINEERING

SEOUL NATIONAL UNIVERSITY

Abstract

Phosphate removal in water is a critical issue because excess levels of it can cause severe eutrophication. The conventional method for phosphate removal, such as chemical precipitation, activated sludge, and adsorption, have suffered from generating additional waste caused by the usage of excessive chemicals, and unavoidable sludge production. Capacitive deionization (CDI) has considered an alternative technology by environmental benign characteristics, high energy efficiency, and simple operation based on charge/discharge. These advantageous features are allowed by achieving ion separation based on fundamentals of electrochemistry. However, the conventional CDI suffers from a lack of selectivity for phosphate, resulting from non-selective anion removal of positively biased electrodes.

In this dissertation, a novel CDI system for the phosphate removal was suggested by adopting phosphate selective adsorbent as an electrode material. This CDI system consisted of layered double hydroxide and recued graphene oxide composite (LDH/rGO) electrode and nickel hexacyanoferrate (one of Prussian blue analogues, PB) electrode with cation exchange membrane.

LDH/rGO-PB system showed superior phosphate removal compared to conventional CDI system in the presence of excess chloride ion. In addition, this system showed selective behavior for phosphate removal allowing maintained the phosphate removal efficiency when chloride concentration increased 20 times higher than phosphate concentration. It was attributed to ligand exchange reaction and intercalation between phosphate and LDH part of LDH/rGO electrode, which are mainly assisted by capacitive behavior. The phosphate selective removal of this LDH/rGO-PB system was also exhibited in the real water matrix (Han River, Seoul, Korea) indicating high potential for practical application.

Second, the strategy of thermal treatment to enhance the performance of LDH/rGO electrode was investigated. Thermally treated LDH/rGO (tLDH/rGO) allowed increasing active sites of LDH resulted from elimination of intercalated anions (nitrate) and water molecules. With tLDH/rGO electrode as phosphate capturing electrode, excess activated carbon electrode covered cation exchange membrane was used for cation capturing (tLDH/rGO-AC system). In tLDH/rGO-AC system, the phosphate adsorption capacity was increased from 0.4 $mmol \cdot g^{-1}$ to 0.9 $mmol \cdot g^{-1}$ for 1 mM of phosphate at neutral pH without loss of selective property. This increasing capacity was supported by the galvanostatic charge/discharge

measurement, which showed that LDH/rGO electrode capacity was enhanced approximately 60% after thermal treatment. In addition, phosphate enrichment was conducted during releasing step (electrode regeneration step) as a pre-treatment process for phosphate recovery as struvite. With selective property and enrichment application of releasing step, tLDH/rGO-AC system showed the great potential as effectiveness strategy to phosphate removal/recovery.

Keywords: Electrochemical water treatment system; Capacitive deionization; Layered double hydroxide; Reduced graphene oxide; Phosphate removal; Phosphate recovery

Student number: 2015-30207

Table of Contents

LIST OF FIGURES

List of Tables

1. Introduction

1.1. Research Background

Phosphorous is a major nutrient source for growing organism including from microorganism to human. However, when excessively present in water, it causes excessive growth of microorganisms leading eutrophication, one of the most widespread global water quality problems. In England and Wales, the potential economic damage from eutrophication was estimated to be about $105-106 million annually (Pretty, Mason et al. 2003). For this reason, technologies for regulating phosphorous in water (phosphorus exists as phosphate in water) to the appropriate level have been developed in water treatment. As conventional technologies, chemical precipitation and biological treatment have been widely used, and adsorption process is also considered as a phosphate removal technology. However, these conventional technologies have a limitation of causing secondary pollution. A large amount of chemical is required in chemical precipitation and regeneration process for adsorbent, and excess sludge production is critical issue in biological treatment. Furthermore, in the aspect of sustainable development which is selected Agenda of UN for 2030, an additional post-treatment process is

required for phosphate recovery in these conventional phosphate removal technologies.

Capacitive deionization (CDI) has been considered an alternative technology due to its eco-friendly, energy efficient, and simple operation based on charging/discharging. In a conventional CDI process, ions can be captured from an aqueous phase by a simple electrostatic interaction between ions and electrode surface through the electrical double layer (EDL) formation on the electrode surface. It indicates that CDI has been suffered from selective phosphate removal, even though the selectivity should be considered in real applications. For this reason, developing a new approach for selective phosphate removal in CDI process is necessary.

To enhance selective property toward for phosphate in CDI, applying a modified electrode can be one of good approaches. Layered double hydroxides (LDHs) is known as phosphate selective adsorbent consisted of stacked metal hydroxide sheets. Corner-shared metal hydroxide octahedral units form a sheet with di- or tri-valent metals are located at a center of each octahedral units. The sheet of LDH has a positive charge due to tri-valent metal atom leading incorporated anions at interlayer between sheets for charge neutrality. These intercalated anions between LDH sheets are

exchangeable with other anions placed outside of LDHs, which is fundamental principle of LDHs as an adsorbent. Exchange capacity can be limited by intercalated carbonate due to strong affinity between carbonate and LDHs (Chitrakar, Tezuka et al. 2005).

Generally, the pristine LDHs has a poor electrical conductivity resulting in limited charge transfer processes and suppressed electrochemical performance. In order to improving the electric conductivity of LDHs as an electrode material, LDHs are prepared as composite structure with conductive material, such as carbon nanotubes (CNTs), reduced graphene oxide (rGO), and other metallic substrates (Yu, Shi et al. 2014, Sun, Zhang et al. 2018). In addition, electrical conductivity of LDHs is enhanced by exfoliation allowing shorten electron transfer distance (Song and Hu 2014). The composite materials with exfoliated LDHs and conductive substrate have been used as a catalysis for OER and electrode in energy storage systems (Long, Yang et al. 2017). For electrochemical phosphate removal, MgAl-LDH and activated carbon (AC) composite electrode and graphene oxide (GO) intercalated MgMn-LDH composite electrode were reported in electrochemical system (Lai, Liu et al. 2019, Zhu, Hong et al. 2019). However, AC and GO substrate was not sufficient to enhance electrical conductivity of MgAl-LDH showing negligible electrochemical activity in cyclic voltammograms.

1.2. Objectives

In this dissertation, a novel CDI system for phosphate selective removal/recovery was suggested by utilizing the composite electrode of ZnAl-LDH and rGO (LDH/rGO). In this composite structure of LDH/rGO, the affinity of LDH part toward phosphate is playing a role with enhanced electrical conductivity leading electron transfer reaction between phosphate and LDH/rGO electrode.

First of all, the selective performance of LDH/rGO-PB system is examined in mixed solution of phosphate and excess chloride. In this system, nickel hexacyanoferrate (one of the Prussian bleu analogue, PB) is used with a cation exchange membrane as a cation capturing electrode. The mechanisms of selective removal performance for phosphate was studied based on the morphology and electrochemical properties of LDH/rGO electrode. In addition, this system was tested in the real water matrix (Han River, Seoul, Korea) with adding 0.4 $mg \cdot L^{-1}$ of phosphate in order to confirm the feasibility.

Second, for the practical application, the phosphate adsorption capacity ($mmol \cdot g^{-1}$) is enhanced through thermal treatment of LDH/rGO powder. In this study, the CDI system for phosphate selective removal consisted of thermal treated LDH/rGO electrode and AC electrode with a cation exchange

membrane (tLDH/rGO-AC system). In order to understand the influence of thermal treatment, the structural changes of LDH/rGO was investigated along with temperature of thermal treatment process. The phosphate removal performance of thermal treated LDH/rGO electrode was examined in the comparison with pristine LDH/rGO electrode. Capacity of electrode was investigated by electrochemical analysis methods and results of CDI performance in constant voltage mode, and selectivity of the CDI system was tested against with mixed solution of phosphate, nitrate, chloride, and sulfate (1 mM for each anions) at neutral pH in constant current mode. Finally, phosphate enrichment process was suggested by collecting released phosphate from LDH/rGO electrode during discharging process in this system for preventing secondary pollutant production.

2. Literature Review

2.1. Importance of Phosphate

2.1.1. Phosphate as Essential Resource

Almost of phosphorus (phosphorus existed in water as phosphate) is stored in phosphate rock, and this was listed in Critical Raw Material (CRM) of EU from 2017. The material in CRM was selected based on assessment in the aspects of supply risk and economic importance. The major consumption of phosphate rock occur in agriculture at a global rate of around 20,000,000 metric tonnes per year as fertilizers, while the amount of phosphate rock is limited without any alternative resources because phosphorus is the element (Mayer, Baker et al. 2016). On the same lines, there has been warning-predictions that the phosphate rock could be exhausted within 100 years without any actions (Steen 1998, Smil 2000, Gunther 2005, Cordell, Drangert et al. 2009). Furthermore, localization of existed phosphate rock in world allows political and economic risks for many countries. In this situation, phosphate recovery in water has been regarded as one of solution leading a completion of phosphorus resource cycle (Rittmann, Mayer et al. 2011). It is a critical issue when consider that the almost of consumed phosphorus is

releasing into water system through various pathway (Cordell, Drangert et al. 2009).

2.1.2. Phosphate as Harmful Substance Causing Eutrophication

Since phosphate is one of nutrient substances, microorganism in water including algae can bloom when phosphate concentration is excessive. The algal bloom in water system causes eutrophication leading not only a severe ecological damage but also substantial economic problems and latent risks to human health (Mayer, Baker et al. 2016). Phosphate is discharged by various pathway, such as a waste in mining process, animal manure, detergents, and etc. In wastewater plant, the removal of discharged phosphate is conducted mainly by chemical precipitation or activated sludge process resulting in sludge production. In order to deal with this sludge, landfill or calcination is the final process to complete phosphate treatment process, which means unique resource as a biological nutrient has lost without any recovery processes.

2.2. Capacitive Deionization as Alternative Technology

2.2.1. Limitation of Conventional Phosphate Removal Technologies

As conventional technologies for phosphate removal, chemical precipitation and biological treatment (activated sludge) are widely used in wastewater plant. In chemical precipitation process, phosphate removal can be conducted by addition of chemicals, such as alum, iron salts, and lime (Fytianos, Voudrias et al. 1998). The limitations of chemical precipitation are ineffective for a low initial concentration of phosphate, and requirement of excess amount of chemicals to achieve safe range of concentration in effluent (Figure 1 and Figure 2). On the other hand, biological treatment is a sensitive process resulting in unstable efficiency (Sun, Yang et al. 2017). The most critical issue of biological treatment is a waste sludge disposal leading cost problem of wastewater treatment (Neufeld and Thodos 1969, Yang, Wang et al. 2018). Finally, although adsorption process has been regarded as cost effective process with high efficiency compared to other technologies, the production of large amount of sludge (used adsorbents) is inevitable causing the requirement of post-treatment (Jin, Zhang et al. 2018). Moreover, when consider about regeneration of adsorbents, strong chemical, 1 M of sodium hydroxide normally, would be used for this process, which is also secondary pollution production.

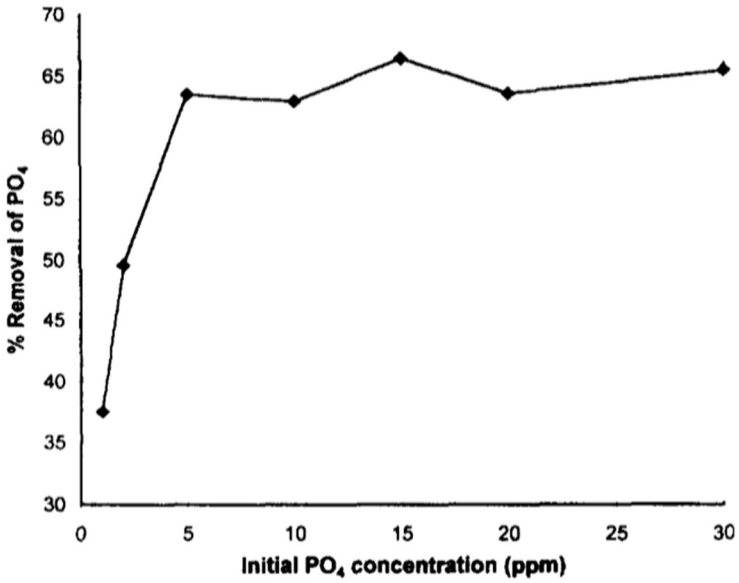

Figure 1. Effect of initial phosphate concentration on removal efficiency of phosphate in chemical precipitation process using $FeCl_3 \cdot 6H_2O$ (Fytianos, Voudrias et al. 1998).

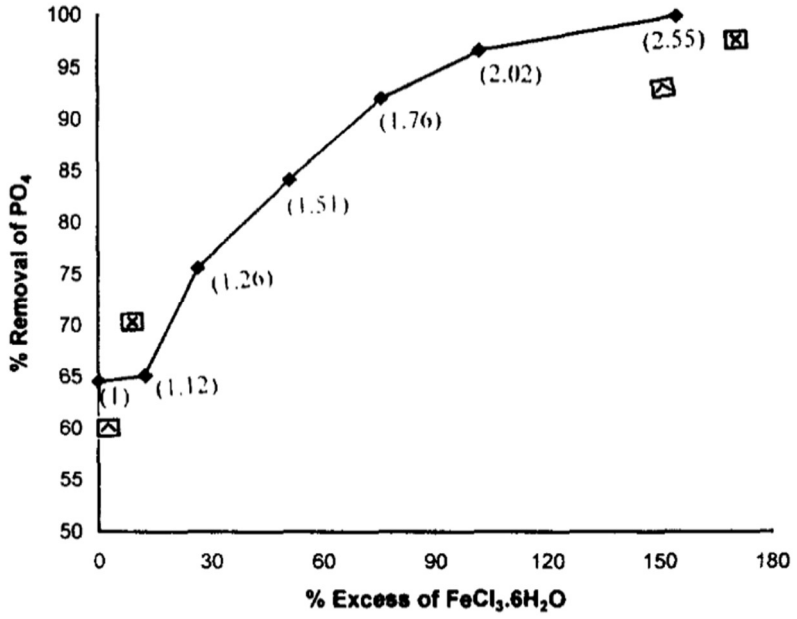

Figure 2. Effect of excess of ferric ion salt ($FeCl_3 \cdot 6H_2O$) on phosphate removal performance. Values in bracket indicates the ratio of Fe:P (Fytianos, Voudrias et al. 1998). In order to achieve high removal efficiency, the larger amount of ferric ion salt was required.

2.2.2. Capacitive Deionization

CDI was originated from electrochemical de-mineralization technology consisted of porous carbon electrodes in 1960s (Blair and Murphy 1960). As similar with de-mineralization, activated carbon has been widely used as electrodes in CDI indicating that CDI is operated by identical principle of EDL storage with de-mineralization. Based on EDL principle, CDI has gained attraction as a next generation technology for desalination due to its environmentally benign, high water recovery, and high energy efficiency characteristics.

Although, in general, CDI is composed of a pair of nanoporous carbon electrode and separator to providing water flow channel with preventing short circuit, CDI has been developed by adopting electrode from energy storage systems. For example, the salt adsorption capacity (SAC) was highly improved from 13.5 $mg \cdot g^{-1}$ to 31.2 $mg \cdot g^{-1}$ by utilizing sodium manganese oxide (NMO) electrode with porous carbon electrode and anion exchange membrane as a counterpart(Lee, Kim et al. 2014). It is attributed to different principle of NMO for ion capturing with activated carbon electrode. During charging step, sodium ions are captured by chemical reaction (intercalation) with NMO, whereas chloride ions are stored in the EDL on porous carbon electrode. With the virtue of selective intercalation reaction of various

electrode, such as NMO, sodium iron pyrophosphate ($Na_2FeP_2O_7$), and Prussian blue analogues, the application area of CDI has been extended from desalination to selective ion separation (e.g. selective ion separation, Figure 3) (Kim, Lee et al. 2016, Kim, Yoon et al. 2017, Yoon, Lee et al. 2018).

On the contrast with cations, anion selective separation in CDI is difficult to achieve even though harmful anions should be often concerned in environmental situation. For anion removal, there no specific ion separation, but only trends of anions electrosorption on carbon surface were reported (Zafra, Lavela et al. 2013, Chen, Zhang et al. 2015). There are several factors to determine anion affinity in electrosorption, such as hydrated radius, ion size, and valence state. However, the exact effect of these factors on anion selectivity is still ambiguous with some controversial results. When carbon electrodes were used in CDI, for instance, the selective behaviors were displayed with inconsistency for monovalent ion compared to divalent ion (Hou, Taboada-Serrano et al. 2008, Sun, Chai et al. 2018). As shown in Figure 4, recently, the study of electronegativity effect on anion selectivity was reported with comparison among Cl^-, ReO_4^-, SO_4^{2-}, and NO_3^- resulting in strongly dependence based on modeling (Sun, Chai et al. 2018).

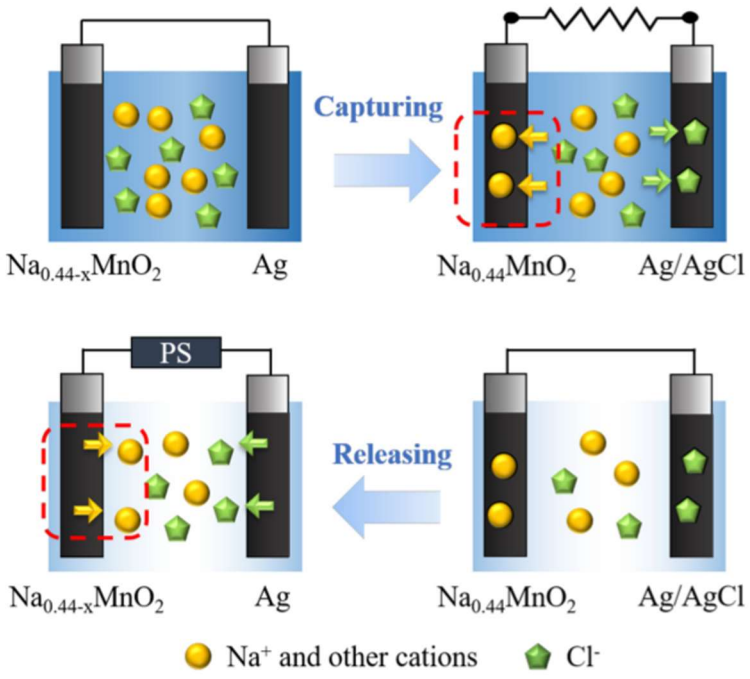

Figure 3. Scheme of $Na_{0.44-x}MnO_2$/Ag in CDI system for selective ion separation (Kim, Yoon et al. 2017). With sodium manganese oxide electrode, CDI system can be applied for selective ion separation.

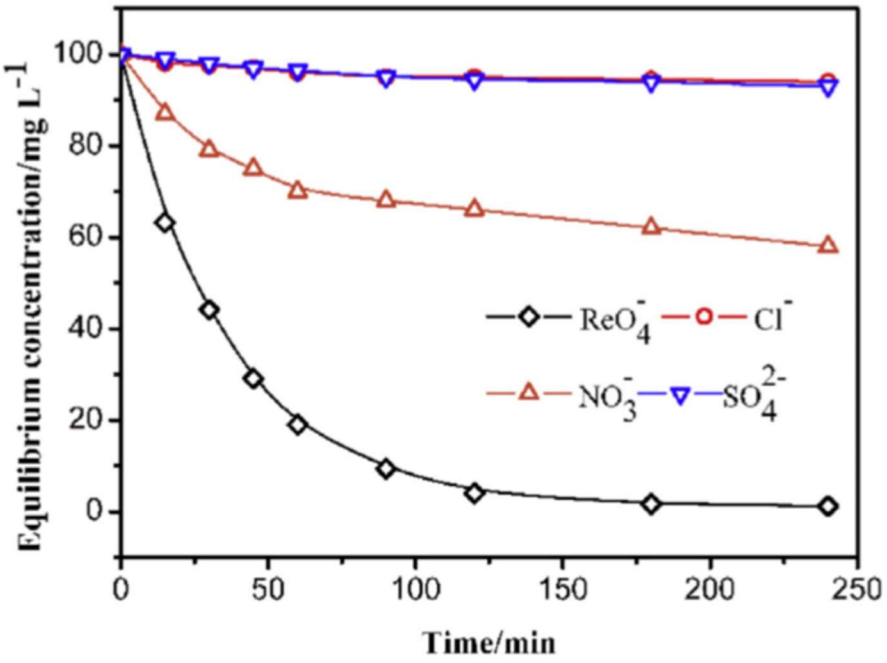

Figure 4. Concentration profiles of CDI effluent in mixed solutions. For all anions, concentrations were all 100 mg·L^{-1} at pH 2, and 25 ℃ (Sun, Chai et al. 2018). The descending order (ReO_4^- > NO_3^- > Cl^- = SO_4^{2-}) was depend upon electronegativity.

Despite the lack of selectivity of porous carbon electrode toward anions, CDI has been studied for nutrient removal including nitrogen (N) and phosphorus (P) removal from aqueous phase. After biological treatment in wastewater plant, the effluent would have a suitable ion concentration for CDI operation. Nevertheless, for the most of cases, nutrient species exist with other competing anions which are higher concentration than target ions. Therefore, the selective property toward target ion is essential to achieve effective CDI process in nutrient removal. For example, with various carbon based electrode which separate ion from water via EDL storage principle, CDI system showed non-selective behavior for nutrient species removal in the presence of other competing ions (Figure 5) (Tang, Kovalsky et al. 2015, Huang, He et al. 2017, Pastushok, Zhao et al. 2019). In order to use activated carbon electrode in CDI for nutrient removal including phosphate, pre-treatment is required to reduce or eliminate competing ions from water.

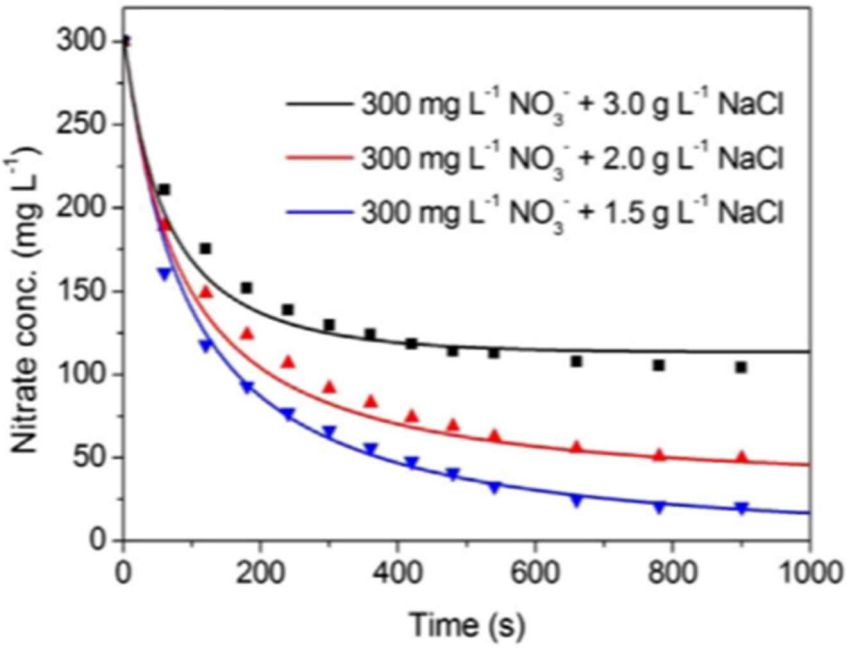

Figure 5. Nitrate removal with effect of chloride ion in batch-mode CDI process (Tang, Kovalsky et al. 2015). Activated carbon electrode was used in this system. Nitrate removal efficiency was decreased along with increasing chloride concentration indicating the lack of selectivity for nitrate.

2.3. Layered Double Hydroxide

2.3.1. Layered Double Hydroxide as Selective Adsorbent

LDH has been studied as anion adsorbent due to its unique property which is originated from structural features. As shown in Figure 6, LDH is composed of two metal cations including div- and trivalent which are octahedral coordination with hydroxides. These octahedral units are sharing corners providing a sheet which has positive charge due to trivalent metal cations. Anions with water molecules are intercalated at interlayer space to neutralize charge, and these anion are exchangeable with other anions placed at outside of LDH. Because this unique property, LDHs have been studied as an anion exchangeable adsorbent.

There are several factors that affect the adsorption capability and selectivity of LDHs, based on the characteristics of LDH itself. The ratio of divalent and trivalent metal cations is one of major factor determining charge density of a LDH sheet. For example, in Figure 7, arsenite adsorption capacity for MgFe-LDH was decreased as increasing the ratio of Mg to Fe of LDH (Cao, Guo et al. 2016). However, for phosphate removal, adsorption capacity of ZnAl-LDH was changed depending on Zn/Al ratio, but without any clear tendency (Cheng, Huang et al. 2009). The effect of metal cation species in LDHs on

the adsorption capacity also reported. As displayed in Figure 8, Xiang Cheng *et al,* compared phosphate adsorption capacity of LDHs contained different metal species with identical ratio of M^{2+} and M^{3+}, which are fabricated by same procedure. Depending on the metal cation, adsorption capacity was varied from 5 mg-P·g^{-1} to 25 mg-P·g^{-1} (Cheng, Huang et al. 2009).

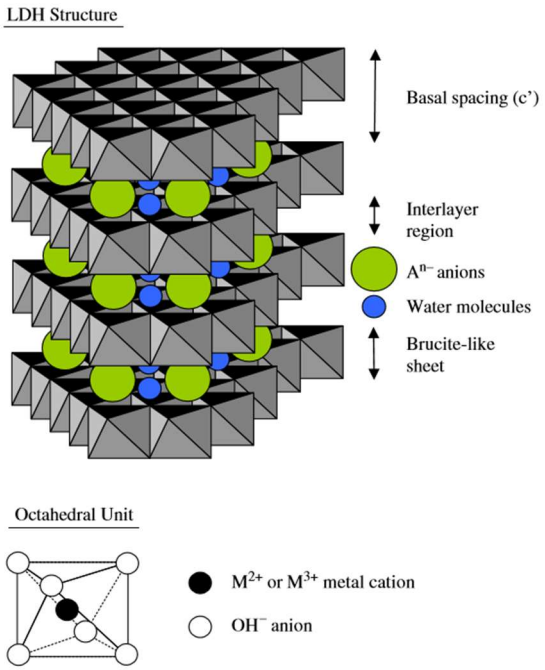

Figure 6. Schematic of LDH structure (Goh, Lim et al. 2008).

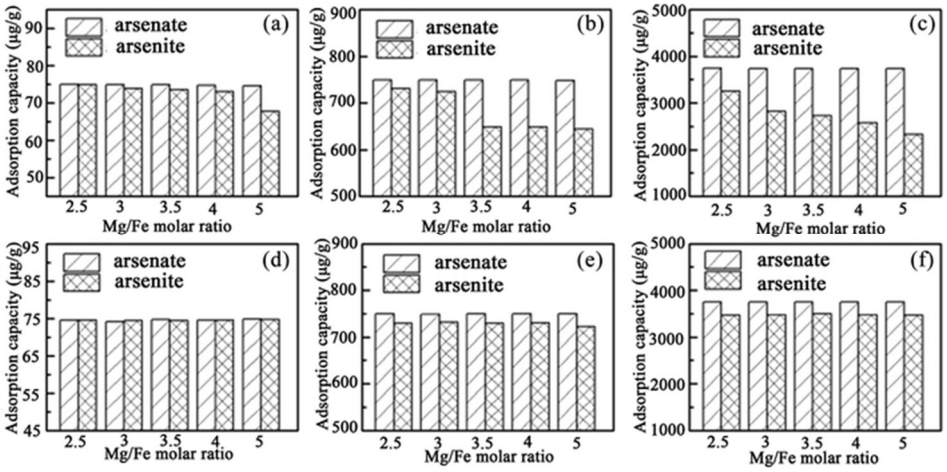

Figure 7. Adsorption results of uncalcined (a-b) and calcined (d-f) MgFe-LDH for arsenic species (Cao, Guo et al. 2016). Total arsenic concentrations are 150, 1500, and 7500 $\mu g \cdot L^{-1}$ for a and d, b and e, and c and f, respectively. The adsorption capacity of arsenite was decreased for uncalcined and calcined MgFe-LDH according with the ration of Mg to Fe was increased.

Selective properties of LDHs are widely studied for various anions including chloride, nitrate, sulfate, phosphate, arsenate, and so on. In various studies which reported the order of anion selectivity based on experimental data, carbonate is most powerful anion to interact with LDHs. Arsenic and phosphate showed also strong affinity with almost of species of LDH indicating that physiochemical property of anion is also important to achieve selective removal (Goh, Lim et al. 2008, Islam and Patel 2010, Wang, Zhang et al. 2018). For MgMn-LDH, the selectivity order was investigated by measuring equilibrium distribution coefficient (K_d) resulting in $Cl^- < NO_3^- < SO_4^{2-} << HPO_4^{2-}$ (Tezuka, Chitrakar et al. 2004). In ZnAl-LDH case, the selectivity order is $Cl^- < HCO_3^- < SO_4^{2-} < PO_4^{3-}$ was determined by adsorption capacity in 10 mM of each anion at pH 7 (Hatami, Fotovat et al. 2018). Calcined MgAl-LDH showed adsorption capacity for anions in pH 10 as following order: $NO_3^- < Cl^- < SO_4^{2-} << AsO_4^{3-} < PO_4^{3-}$ (Morimoto, Anraku et al. 2012). According to this study, arsenic and phosphate formed inner-sphere complexes through ligand exchange reaction, while the others were adsorbed by electrostatic interaction.

Adsorbed phosphate is difficult to desorb from LDH due to its strong interaction with LDH. Additionally, the desorption rate is very slow taking a few days. With 5 M NaCl and 0.1 M NaOH mixed solution, phosphate

desorbed from calcined MgMn-LDH as 82% of adsorbed phosphate during 3 days (Chitrakar, Tezuka et al. 2005). For MgAl-LDH, only 80% of phosphate desorbed under 5 M NaOH solution during 1 day (Kuzawa, Jung et al. 2006). In neutral pH, phosphate was desorbed only ~30% from ZnAl-LDH in the presence of nitrate during 100 h (above 4 days) indicating chemisorption of phosphate with partial reversibility (Hatami, Fotovat et al. 2018). Although phosphate desorption was studied with various composition of desorption solutions (Table 1), regeneration of ZnAl-LDH adsorbent was remained as challenging issue due to leaching of metal cations in harsh desorption condition.

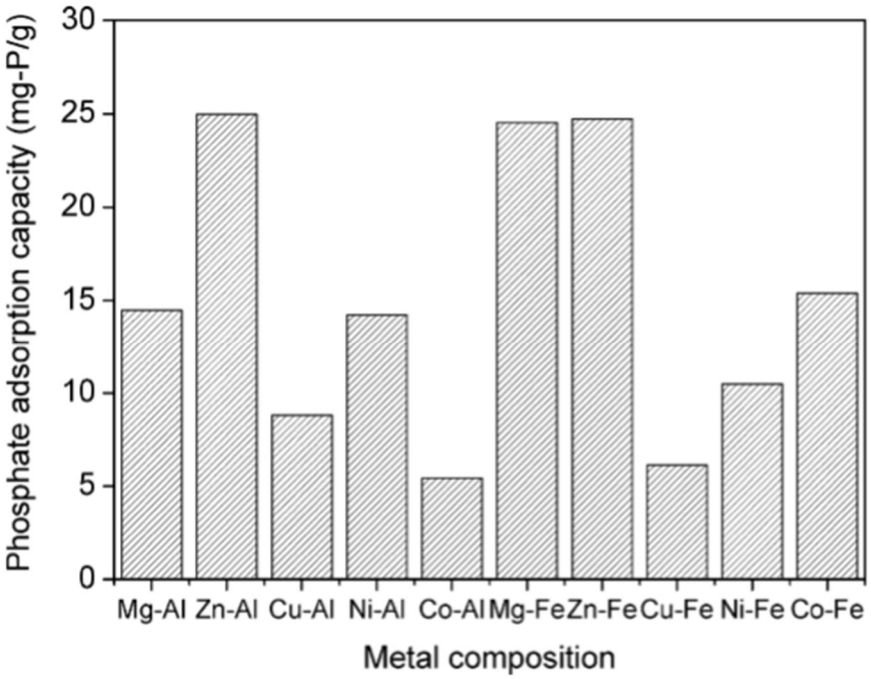

Figure 8. Effect of metal species in LDHs on phosphate adsorption from sewage sludge filtrate (Cheng, Huang et al. 2009). Capacities were varied depending on metal species.

Table 1. Desorption result of phosphate from ZnAl-LDH (Cheng, Huang et al. 2009).

Desorption solutions	Desorption (%)	Zn^{2+} ($mg \cdot L^{-1}$)	Al^{3+} ($mg \cdot L^{-1}$)
1% (w/v) NaOH	20.58	23.90	16.75
2% (w/v) NaOH	37.99	54.00	34.18
3% (w/v) NaOH	52.27	65.40	33.70
5% (w/v) NaOH	87.57	85.00	36.12
10% (w/v) NaOH	89.34	333.10	61.17
20% (w/v) NaOH	91.24	426.60	66.12
5% (w/v) NaCl	7.56	3.20	30.51
10% (w/v) NaCl	10.34	8.70	30.49
20% (w/v) NaCl	21.17	9.50	30.19
5% (w/v) $NaCO_3$	40.31	41.34	20.11
10% (w/v) $NaCO_3$	84.22	100.35	43.06

2.3.2. Electrochemical Application of Layered Double Hydroxide

LDHs have various applications as well as adsorption, such as catalysis, biology, and energy storage due to the unique properties including 2D structure with positive charge, tunable metal cations without significant disordered structure, and wide range of intercalation reaction by flexible interlayer distance (Seftel, Popovici et al. 2008, Parida, Sahoo et al. 2010, Cho, Jang et al. 2013, Song and Hu 2014, Yu, Shi et al. 2014, Zhang, Xu et al. 2014, Long, Yang et al. 2017). For electrochemical application, there are many approaches to fabricated LDH based electrode with overcoming poor electrical conductivity. The purpose of these various method is to obtain well dispersed LDH on the conductive substrate indicating that aggregation of LDH cause less conductive property with providing long distance for electron transfer. As shown in Figure 9, single LDH sheet is suitable for electrochemical application with reducing electron transfer distance, which can be prepared by exfoliation of bulk LDHs (Song and Hu 2014). As a conductive substrate, carbon based materials including CNTs and reduced graphene oxide, and conductive metal foams are widely used to enhance electrical conductivity of LDHs. The metal composition of LDHs are also considered as important factor of electrochemical performance. For example, in electrocatalytic reactions, Ni, Co, Fe, and Zn are famous transition metal

cation for LDHs showing excellent performance for oxygen evolution reaction (OER)(Shao, Zhang et al. 2015). However, the study of relation between metal composition and OER performance of LDHs is needed to better understanding.

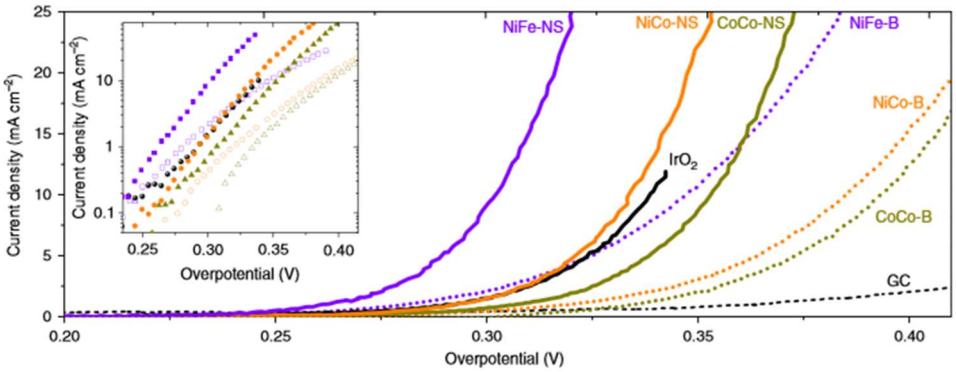

Figure 9. Electrochemical behavior of LDHs compared to IrO_2 nanoparticles (Song and Hu 2014). 'NS' indicates nano sheet obtained from LDHs, and 'B' indicates bulk LDHs. NiFe-LDH (in here, NiFe-NS) showed best performance with lowest overpotentials for oxygen evolution reactions.

3. Phosphate Removal by Electrochemical System using Phosphate Selective Electrode

3.1. Introduction

A tremendous amount of phosphorus from various human activities, such as the use of pesticides, detergents, and manure, has been released into aquatic environments as a phosphate in wastewater. Excess levels of phosphate in water environments cause ecological damage through the process of eutrophication, one of the most widespread global water quality problems, leading to substantial economic problems and latent risk to human health (Mayer, Baker et al. 2016, Gu, Xie et al. 2017).

In order to control the phosphate concentration in discharge water, various technologies including chemical precipitation, activated sludge, and adsorption processes have been studied. However, chemical precipitation and activated sludge suffer from a sludge disposal problem, and adsorption process is limited by regeneration issue associated with the usage of a large amount of chemicals. Capacitive deionization (CDI) has been considered an alternative technology due to its eco-friendly, energy efficient, and simple operation based on charging/discharging (Kim, Yoon et al. 2017, Lee, Kim et

al. 2017, Yoon, Lee et al. 2019). In a conventional CDI process, ions can be captured from an aqueous phase by a simple electrostatic interaction between ions and electrode surface through the electrical double layer (EDL) formation on the electrode surface. It indicates that CDI has been suffered from selective phosphate removal, even though the selectivity should be considered in real applications. For this reason, developing a new approach for selective phosphate removal in CDI process is necessary (Farmer, Fix et al. 1995, Zafra, Lavela et al. 2013, Macías, Lavela et al. 2014, Chen, Zhang et al. 2015, Huang, He et al. 2017, Ge, Chen et al. 2018).

This study examines a novel electrochemical system consisted of phosphate selective electrode, the ZnAl-layered double hydroxide with reduced graphene oxide (LDH/rGO), and nickel hexacyanoferrate (one of the Prussian blue analogues, PB). The morphology and electrochemical properties of the LDH/rGO electrode were investigated in order to understand its phosphate capturing behavior. The phosphate selective removal performance of the electrochemical process with LDH/rGO and PB electrodes (LDH/rGO-PB system) was examined under various ratios of phosphate to chloride (1:5, 1:10, and 1:20), considering energy consumption and regeneration practice. In addition, the phosphate removal performance of

this system was examined in the real water matrix (Han River, Seoul, Korea) with adding a low level of phosphate (0.4 $mg \cdot L^{-1}$).

3.2. Experimental Section

3.2.1. Reagents and Chemicals

All chemicals were purchased from Sigma Aldrich (St. Louis, MO, USA), and used without further purification. The cation exchange membrane (Selemion® CMV, Asahi Glass Company, Japan) was used as received.

3.2.2. Preparation of Composite Electrode (LDH/rGO Electrode)

The LDH/rGO powder was fabricated by following procedure (Gao, Wang et al. 2011). First, for the preparation of the LDH/rGO powder as active material, rGO was synthesized using Hummers method (Hummers Jr and Offeman 1958). Graphene oxide (GO) powder was immersed in 30 $g \cdot L^{-1}$ of L-ascorbic acid at 90℃ overnight. Then, the resulting rGO was well washed in deionized water and was dispersed in 250 mL of the aqueous solution which contained 0.744, 0.479, and 0.526 g of $Zn(NO_3)_2 \cdot 6H_2O$, $Al(NO_3)_3 \cdot 9H_2O$ and urea, respectively. The LDH/rGO powder was obtained by hydrothermal processing at 95℃ for 24 h.

Prior to fabrication of the LDH/rGO electrode as a freestanding composite electrode, the LDH/rGO powder, conducting agent, and polytetrafluoroethylene (PTFE) were each mixed with weight ratios of 8:1:1. Then, the composite electrode was fabricated by the role-pressing method and dried in a vacuum oven. The pure LDH electrode, without adding rGO, was prepared with the same procedure.

3.2.3. Characterization of LDH/rGO

The LDH/rGO and the pure LDH powders were analyzed with a scanning electron microscope (SEM, JSM-6700F, Jeol, Tokyo, Japan), high resolution transmission electron microscope (HR-TEM, JEM 3010, Jeol, Tokyo, Japan), and X-ray diffractometer (XRD, the Rigaku D-MAX2500, Tokyo, Japan). Additionally, the LDH/rGO electrode was examined by post-mortem analysis with Fourier Transform Infrared Spectroscopy (FT-IR, Cary 600 series FT-IR Agilent Technologies, CA, USA) and XRD analysis after capturing step. For XRD analysis, the capturing step was conducted under a high phosphate concentration (1 M of phosphate) to maximize changes for clear observation.

The electrochemical properties of the LDH/rGO electrode were investigated using cyclic voltammetry (CV) and galvanostatic charge/discharge measurements. These measurements were conducted in a

custom-built cell with installation of the LDH/rGO electrode as a working electrode and excess activated carbon as a counter electrode (Lee, Kim et al. 2017). With Ag/AgCl (saturated KCl) reference electrode, CV was performed in the three electrode system under 2 $mV \cdot s^{-1}$ in of phosphate solution (1 M, sodium phosphate) and chloride solution (1 M, sodium chloride) at a neutral pH, using a potentiostat (PARSTAT 2273, Princeton Applied Research, TN, USA). The galvanostatic charge/discharge was carried out using a battery cycler (WBCS3000, WonA Tech Co, Seoul, Korea) with/without Ag/AgCl (saturated KCl) reference electrode for monitoring potentials of the LDH/rGO electrode.

3.2.4. Evaluation of LDH/rGO-PB system

The semi-batch electrochemical system was prepared with the LDH/rGO as a phosphate capturing electrode, and PB, nickel hexacyanoferrate which is one of the Prussian blue analogues with a cation exchange membrane as cation capturing electrode (Yoon, Lee et al. 2018).

Before the phosphate removal test, the PB was pretreated by applying a constant current of 0.6 $mA \cdot cm^{-2}$ until -1.5 V of the cell potential in 100 mM of potassium nitrate for the activation of PB by releasing cations. The phosphate removal by the LDH/rGO-PB system was conducted by repeating

the two steps up to the 5th cycle inducing electrochemical capturing and release of phosphate (Figure 10). For the capturing step, constant current (0.6 mA·cm^{-2}) with the cell voltage limit of 1.0 V was applied the system with the mixed solution containing 1 mM of phosphate and various concentrations of chloride ranging from 5 mM to 20 mM at neutral pH. In the releasing step, reverse current (-0.6 mA·cm^{-2}) was applied up to -1.5 V of the cell potential in the 10 mM of sodium hydroxide solution. The average values of removal efficiency for phosphate and chloride were estimated from where the process was stabilized. In addition, to express the selective performance of LDH/rGO-PB system, the selectivity coefficient (*S*) was also calculated as follows (Su, Hübner et al. 2017).

$$\text{Selectivity coefficient } (S) = \frac{R_P/C_P}{R_{Cl}/C_{Cl}} \qquad \text{Equation (1)}$$

where C_P (mmol·g^{-1}) and C_{Cl} (mmol·g^{-1}) were the amount of captured phosphate and chloride on the electrode, respectively, and R_P (mmol·L^{-1}) and R_{Cl} (mmol·L^{-1}) were the remaining aqueous concentrations of phosphate and chloride after the capturing step, respectively. Note that the R_p/C_p (L·g^{-1}) and R_{Cl}/C_{Cl} (L·g^{-1}) were the distribution coefficients for phosphate and chloride, respectively.

Energy consumption was calculated based on the area of cell potential vs. charge plot for capturing/releasing steps (Kim, Lee et al. 2015). The samples

were collected when the capturing or releasing step was finished, and the ion concentrations were measured with ion chromatography (DX-120, DIONEX, CA, USA). A conventional CDI system with activated carbon electrode (SX-plus, Norit Activated Carbon, Amersfoort, Netherland) was examined for comparative purposes under the selected condition (1 mM of phosphate and 10 mM of chloride solution).

Instead of 10 mM of sodium hydroxide solution in the releasing step, two different solutions (10 mM of sodium bicarbonate and 10 mM of sodium chloride) were examined. Capturing-releasing steps were repeated at a selected condition (1 mM of phosphate and 10 mM of chloride). From the 1st cycle to 3rd cycle, bicarbonate solution was used. From 4th cycle to 6th cycle, chloride solution was used.

3.2.5. Preparation of Simulated Water using Real Water Matrix

The selective phosphate removal of the LDH/rGO-PB system was examined in the simulated water (Han River, Seoul, Korea), which was prepared by adding 0.4 mg·L^{-1} of phosphate into the Han River water (micro filtered). 10 mM of sodium hydroxide solution was used for the releasing step.

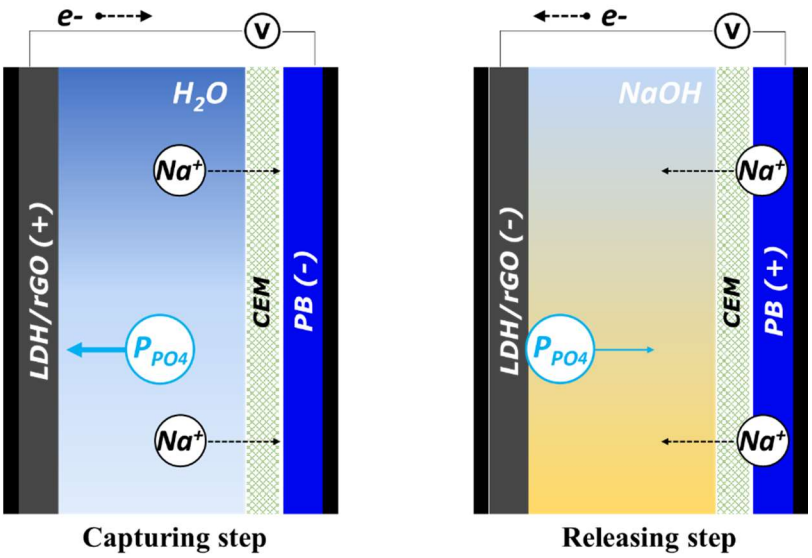

Figure 10. Schematic of LDH/rGO-PB system of capturing/releasing step. Each step was conducted in semi-batch mode. During capturing step, phosphate is captured by negatively biased LDH/rGO electrode and cation (sodium) is intercalated into PB electrode. During releasing step, captured phosphate and sodium are released from each electrode into 10 mM of sodium hydroxide solution.

3.3. Results and Discussion

3.3.1. Characterization of LDH/rGO

Figure 11 shows the XRD patterns (a), the SEM (b) and the TEM images (c) of the LDH/rGO in comparison with those of the pure LDH, respectively. As shown in Figure 11 (a), the LDH/rGO was successfully synthesized with a typical lamella structure of LDHs, which is confirmed by the identical peak positions of (003), (006), (009), (104) and (105) with pure LDH. However, in Figure 11 (b), a well-stacked structure was observed only for pure LDH by SEM image, while it was not clearly shown in the SEM image of the LDH/rGO, indicating that the layered structure was less developed. Considering the poor electrochemical properties of pure LDH due to large inter-layer distance, the less developed layered structure of the LDH/rGO appeared to be superior to pure LDH in terms of electrochemical properties due to a shorter inter-layer distance (Song and Hu 2014, Sun, Zhang et al. 2018). Furthermore, the TEM images of the LDH/rGO in Figure 11 (c) exhibited a graphene layer of the LDH/rGO, while no graphene layer was observed in case of the pure LDH. The graphene layer of the LDH/rGO is presumed to play a role as a conducting substrate leading to improvement in

the conductive property of the LDH (Song and Hu 2014). The structural advantages of LDH/rGO was supported by a larger area of the CV curve compared to that of pure LDH, indicating the improved electrochemical properties (refer to Figure 12)

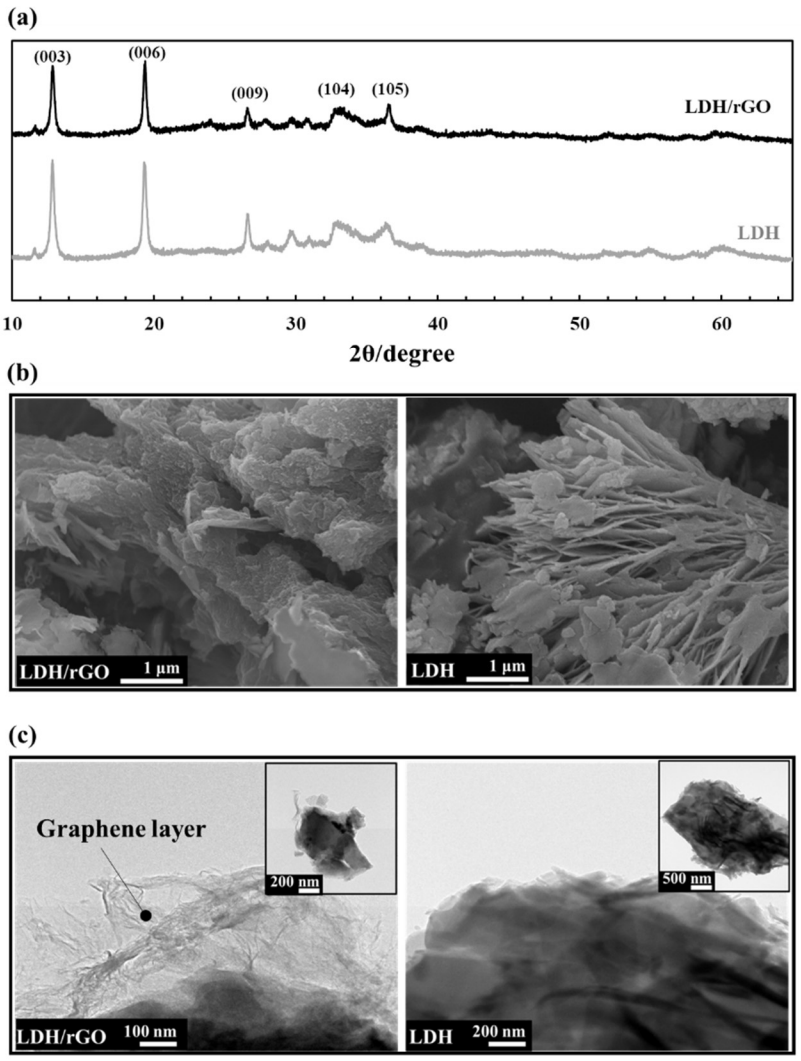

Figure 11. XRD patterns (a), SEM images (b), TEM images (c) of layered double hydroxide/reduced graphene oxide composite (LDH/rGO) in comparison with those of pure LDH as a powder form.

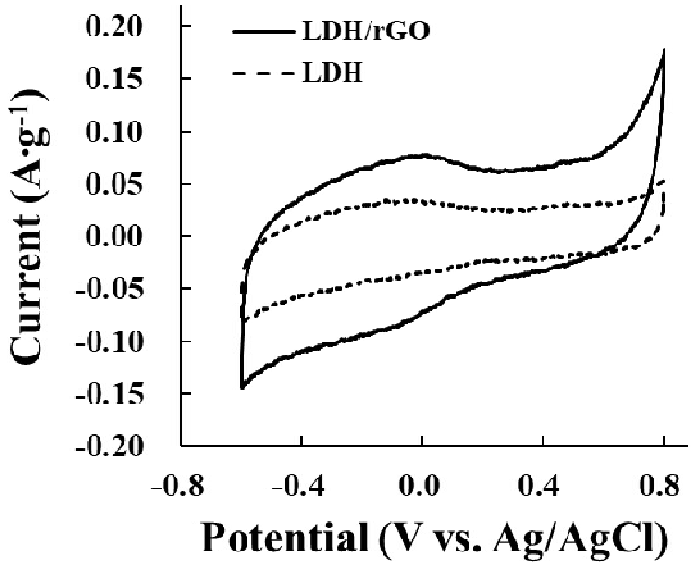

Figure 12. Cyclic voltammograms of layered double hydroxide/reduced graphene oxide composite (LDH/rGO) electrode in comparison with that of pure LDH (2 $mV \cdot s^{-1}$ in 1 M of phosphate buffer solution at neutral pH).

3.3.2. Phosphate Removal Performance of LDH/rGO-PB System

Prior to evaluate phosphate removal performance, potential profiles of LDH/rGO and PB were measured, which is displayed in Figure 13. As shown in Figure 13 (a), during capturing step, the potential of LDH/rGO electrode was increased while the potential of PB electrode was maintained at 0.2 V indicating intercalation reaction of sodium into PB electrode. During releasing step, the potential of LDH/rGO electrode was decreased while the potential of PB electrode was conversed at 0.6 V with de-intercalation of sodium from PB electrode (Figure 13 (b)).

In order to confirm the selective behavior of LDH/rGO-PB system, the comparison with conventional CDI system was conducted. As shown in Figure 15 (a), the *S* coefficient (selectivity coefficient, Equation (1)) for phosphate of electrochemical process consisted of LDH/rGO and PB was around 6 while the electrochemical process consisted of activated carbon electrodes was only around 2. With the *S* coefficient, higher phosphate removal efficiency and lower chloride removal efficiency of LDH/rGO system indicate improved selective performance. Note that when *S* coefficient is greater than 1, the phosphate removal is favorable, compared with the chloride removal at the selected condition. The selective behavior of LDH/rGO system was also examined along with 5 mM, 10 mM, and 20 mM

of chloride with 1mM of phosphate. As shown in Figure 15 (b), the *S* coefficient increased from 2.9 to 7.4 with increase of chloride concentration, indicating the phosphate selective behavior of LDH/rGO-PB system. The high *S* coefficient of LDH/rGO-PB system was attributed to the maintained significant phosphate removal, which decreased only from 54% to 48% even as the chloride concentration of mixture solution increased from 5 mM to 20 mM. Furthermore, the phosphate selective behavior was still observed at pH 5 in Figure 16**,** where phosphate existed as monovalent species, suggesting that the synthesized LDH/rGO exhibited good selectivity for both divalent and monovalent phosphate forms (Morel, Hering et al. 1993, Morimoto, Anraku et al. 2012).

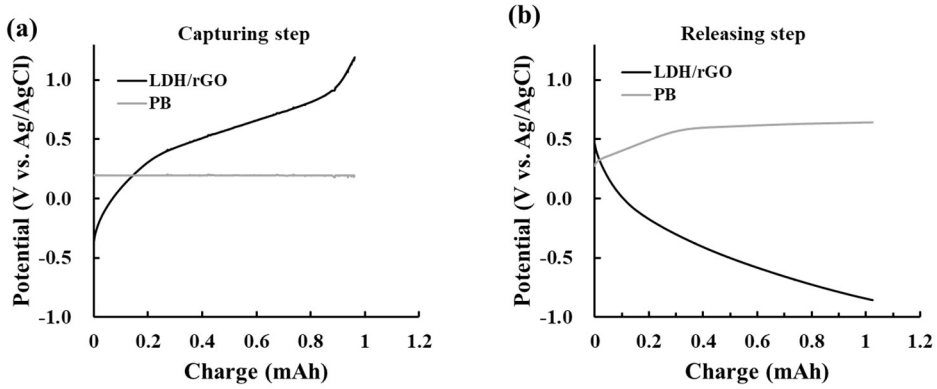

Figure 13. Potential profiles of electrodes in LDH/rGO-PB system. This was measured in 1 mM of phosphate and 5 mM fo chloride for capturing step, and 10 mM of sodium hydroxide solution for releasing step. The cut off voltage for both cases is ±1.5 V at ±0.6 $mA \cdot cm^{-2}$ of current density

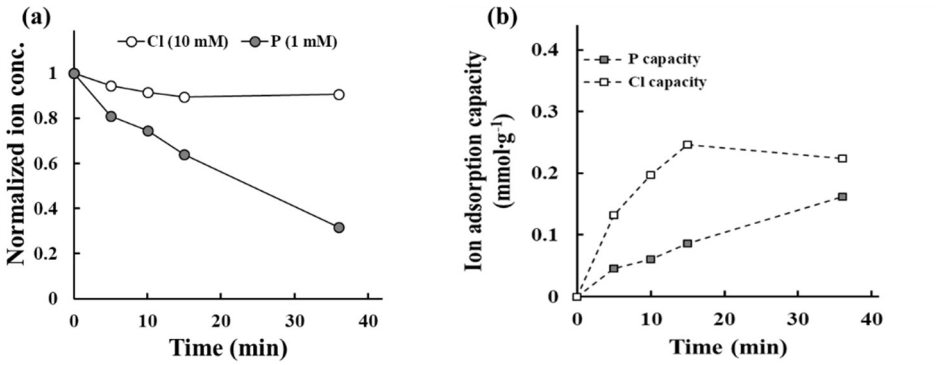

Figure 14. The normalized ion concentration profiles (a) and adsorption capacities (b) during the capturing step in the mixed solution of 1 mM phosphate and 10 mM.

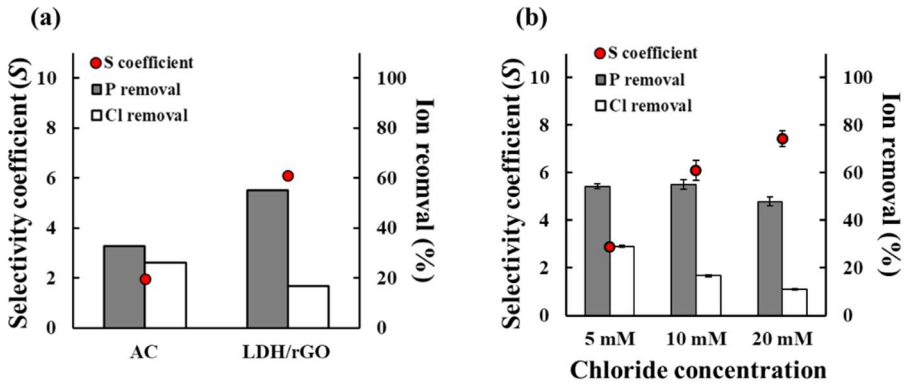

Figure 15. Performance comparison of LDH/rGO-PB system and conventional CDI (a), and phosphate removal performance of LDH/rGO-PB system with various chloride concentrations with 1 mM of phosphate (b). In (a), experiments were performed for 1 mM phosphate and 10 mM chloride mixed solution at neutral pH. Note that the result of LDH/rGO in (a) was duplicated in (b).

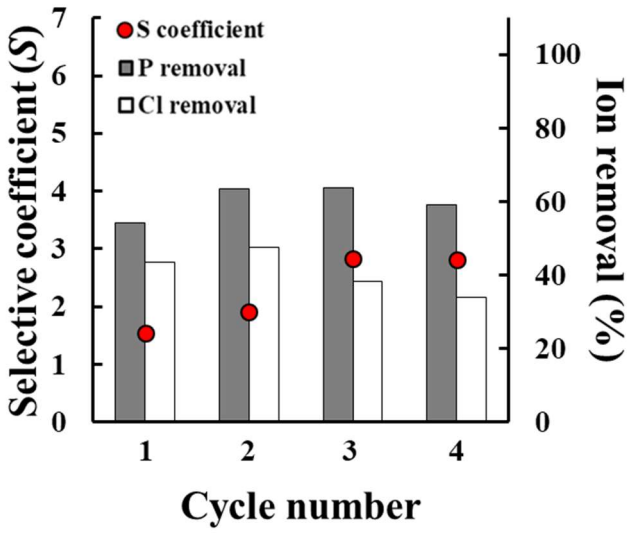

Figure 16. Phosphate removal performance of LDH/rGO-PB system for 1 mM of phosphate and 10 mM of chloride mixed solution at pH 5.

S coefficients were estimated for phosphate (1 mM) and chloride mixed solutions without in Figure 17. Ion removal was conducted for 35 minutes which was similar to the operation time of LDH/rGO-PB system in Figure 15 (b). As shown in Figure 17, *S* coefficients were 7.4, 5.5, and 3.3 along with the chloride concentration 5 mM, 10 mM, and 20 mM, respectively. The decreased *S* coefficient along with increasing chloride concentration indicates an unfavorable selective removal of phosphate when the concentration of competing ion is increased. Please note that this tendency of *S* coefficient is displayed oppositely when the potential was applied to LDH/rGO-PB system in Figure 15 (b). It indicates that the selective removal for phosphate is favorable in the presence of excessive competing ion when an electrical potential is applied. Under the electrical potential, concentrations of ions are increased at electrode surface to form EDL, leading to facilitate adsorption of LDH/rGO with a selectivity towards phosphate which is typical property of LDH.

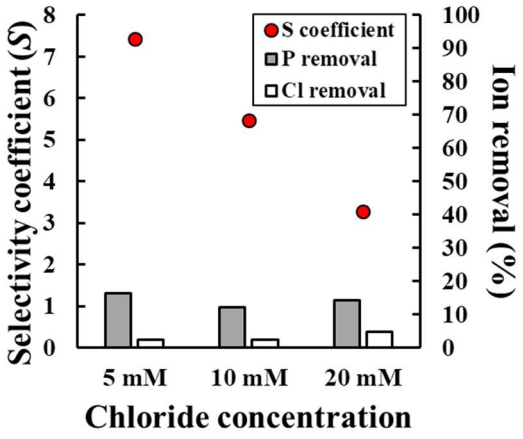

Figure 17. Selectivity coefficient (*S*) of LDH/rGO-PB system for phosphate and chloride mixed solutions without applied potential. Phosphate concentration was 1 mM at neutral pH for all cases.

3.3.3. Energy consumption of LDH/rGO-PB system

The energy consumption of the CDI process using the LDH/rGO was estimated from the area of cell potential profiles vs. charge shown in Figure 18. As shown in Figure 18, the energy consumptions were calculated as 176, 163, and 168 $Wh \cdot m^{-3}$ for the range of 45~55% phosphate removal under three different conditions (5 mM, 10 mM, and 20 mM of chloride with 1 mM of phosphate, respectively). Higher energy consumption in the case of 5 mM of chloride mixture solution (1 mM of phosphate) was caused by higher solution resistance, which was reflected as a higher cell potential profile during the capturing step. The energy consumption of the LDH/rGO-PB system was small compared to the energy consumption of electrocoagulation process (410 $Wh \cdot m^{-3}$ to 22,000 $Wh \cdot m^{-3}$ with 22~100% removal of phosphate) (İrdemez, Yildiz et al. 2006).

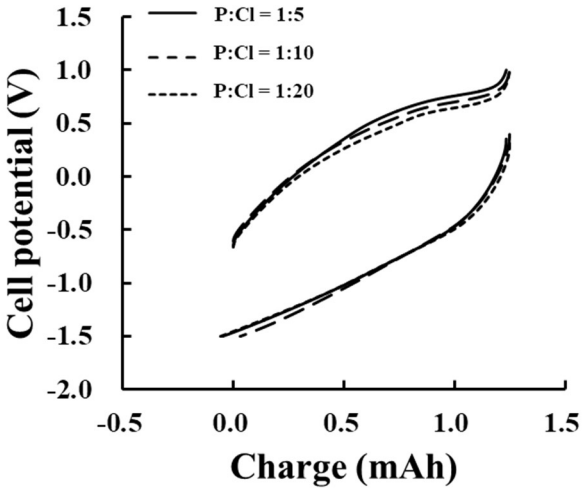

Figure 18. The cell potential vs. charge curves under three different conditions (5, 10, 20 mM of chloride, respectively, with 1 mM of phosphate). Note that the area of the cell potential vs. charge curves indicates the energy consumption for each condition.

3.3.4. Mechanism Study Based on Characterization of LDH/rGO Electrode

In order to understand the selective behavior of LDH/rGO-PB system, electrochemical analysis for LDH/rGO electrode was conducted by the CV curves (a) and galvanostatic charge/discharging curves (b), and the phosphate captured LDH/rGO electrode was analyzed by FT-IR (c) and XRD (d) as shown in Figure 19. In Figure 19 (a), the broad peaks with a red arrow appeared within the potential range from -0.4 V to 0.05 V (vs. Ag/AgCl) in the phosphate solution (1 M), while these peaks were not observed in the chloride solution (1 M). This result implies that LDH/rGO revealed the electrochemical reactions with phosphate, which can be interpreted by b-values of power-law relation for anodic and cathodic processes (0.8 and 0.9, respectively) in Figure 20. Therefore, both capacitive behavior (increasing ion concentration at electrode surface) and electrochemical reactions are thought to be involved to phosphate removal, although it is difficult to understand exact electrochemical reaction between phosphate and LDH/rGO in this study.

As shown in Figure 19 (b), the electron transfer reaction of the LDH/rGO for phosphate was also displayed in the non-linear potential profile of the LDH/rGO. The slope of the potential profile for phosphate was changed near 0 V for anodic process and -0.2 V for cathodic process, leading to the higher

specific capacity for phosphate when compared to chloride (Brousse, Bélanger et al. 2015, Kim, Hong et al. 2015, Yang, Kao et al. 2018). Additionally, as shown in Figure 21, the LDH/rGO electrode exhibited high cyclability in the phosphate solution with coulombic efficiency near unity and retained 71% of the initial discharge capacity after 100 cycles.

The capturing phosphate mechanisms of the LDH/rGO can be explained by the inner-sphere complexation (Figure 19 (c)) and anion intercalation (Figure 19 (d)) of phosphate and the LDH/rGO. As shown in Figure 19 (c), the occurrence of inner-sphere complexation was observed by P-O stretching vibration peak around 1000 cm^{-1} after capturing step resulting from the formation of mono/bidentate complexes (Morimoto, Anraku et al. 2012, Yang, Yan et al. 2014). In the XRD pattern of Figure 19 (d), new peaks appeared at higher 2 theta degree of (003) and (006), respectively, after capturing phosphate, which indicates that phosphate was intercalated into an interlayer of LDH with decreasing interlayer distance (Khaldi, Badreddine et al. 1998, Morimoto, Anraku et al. 2012). Therefore, phosphate can be captured via ligand exchange and intercalation reactions under electrical potential.

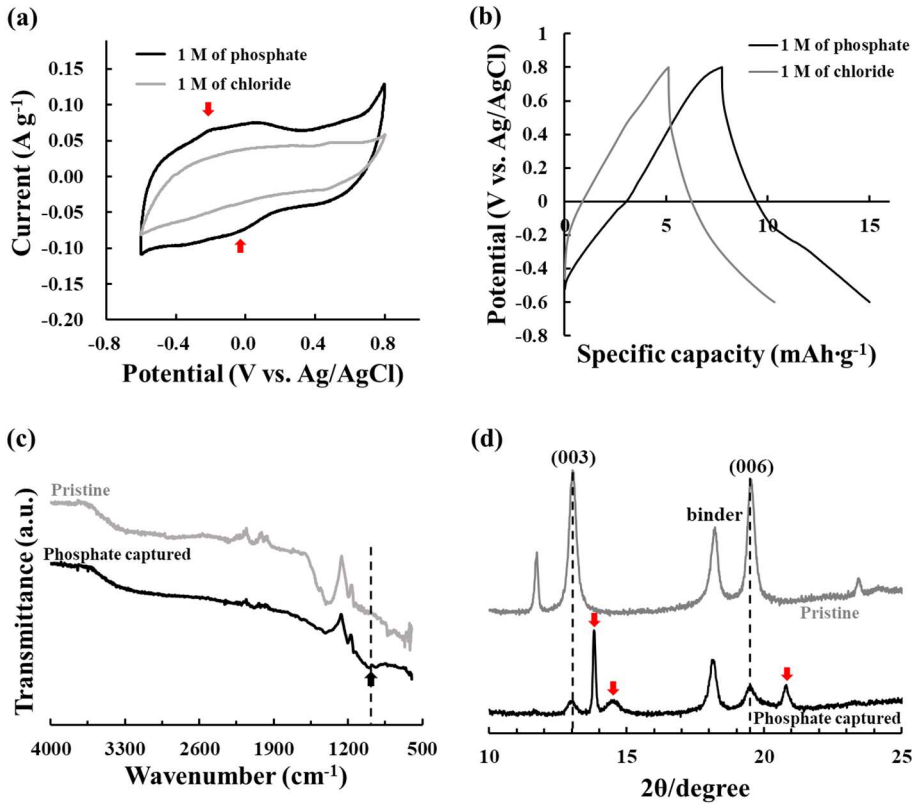

Figure 19. Cyclic voltammograms (a) and galvanostatic charge/discharge curves (b) of LDH/rGO electrode in phosphate (1 M) and chloride solution (1M), respectively, and the FT-IR spectra (c) and the XRD patterns (d) of pristine and phosphate captured (after capturing step) LDH/rGO electrode. The FT-IR was conducted with the phosphate captured LDH/rGO prepared in 1 mM of phosphate and 5 mM of chloride, and the XRD was measured with the phosphate captured LDH/rGO prepared in 1 M of phosphate solution.

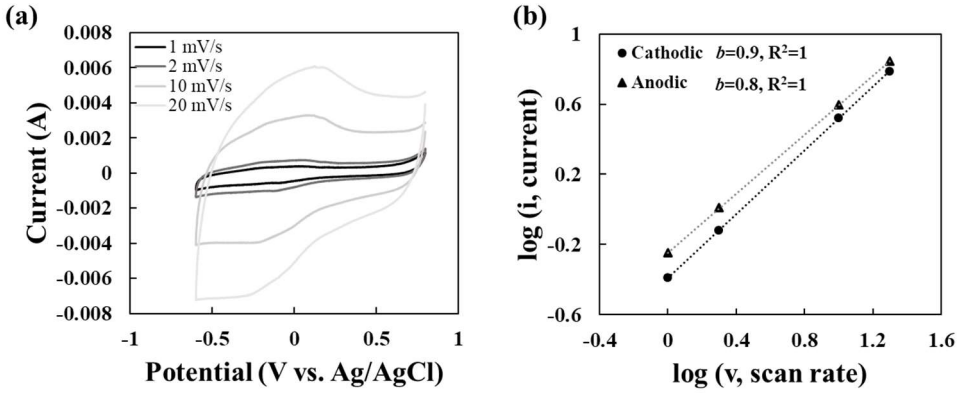

Figure 20. Cyclic voltammograms of LDH/rGO in 1 M of sodium phosphate with various scan rates from 1 to 20 $mV \cdot s^{-1}$ (a), and power-law relation for cathodic and anodic processes between peak current and scan rate (b). The *b* values of the power-law relation were estimated from CV curves of (a) ($\boldsymbol{i} = \mathbf{a} \times \boldsymbol{\nu}^{\boldsymbol{b}}$, where *i* is the current, ν is the scan rate, and a and *b* are adjustable values, respectively, for anodic and cathodic processes).

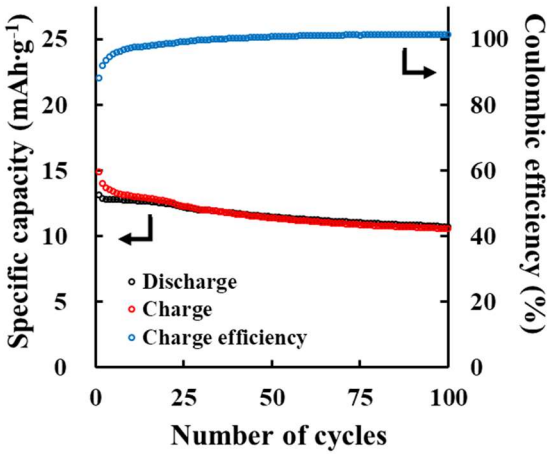

Figure 21. Specific capacity and charge efficiency for 100 cycles of LDH/rGO electrode for charging and discharging steps at neutral pH (100 mM of phosphate ions at ±0.6 mA·cm^{-2}).

3.3.5. Examination of Several Regeneration Solutions during Releasing Step

Figure 22 displays the *S* value of LDH/rGO in the CDI process at two different regeneration solutions for the releasing step. Bicarbonate and chloride solutions were selected because they are more environmentally benign chemicals than hydroxide solution. Sodium bicarbonate (10 mM) was used as a regeneration solution up to 3th cycle, and sodium chloride (10 mM) was used from 4th cycle to 6th cycle. Although the phosphate removal efficiency gradually decreased with the use of bicarbonate and chloride solutions, the phosphate selective performance showing the *S* value above 4.0 was still observed.

3.3.6. Application of LDH/rGO-PB system in the Simulated Real Water Matrix

Figure 23 presents the phosphate removal performance of LDH/rGO-PB system in the simulated water which was prepared by adding about 0.4 mg·L^{-1} of phosphate into Han River water (Seoul, Korea, refer to Table 1 for anion composition). As an example, this phosphate concentration is similar to the wastewater treatment plant in Goyang, Korea. As shown in Figure 23, in spite of very low phosphate concentration in the real water matrix, the LDH/rGO-PB system successfully achieved the selective phosphate removal. The

concentration of phosphate was decreased from 0.4 $mg \cdot L^{-1}$ to 0.009 $mg \cdot L^{-1}$ (the target concentration of phosphate of waste water treatment plant: 0.1 $mg \cdot L^{-1}$). This was about 98% removal, while the removal efficiency of other anions was 55%, 28%, and 70% for Cl^-, NO_3^-, and SO_4^{2-}, respectively. These results suggest the LDH/rGO-PB system has an excellent selective phosphate removal performance, as compared to other anion species in real water matrix.

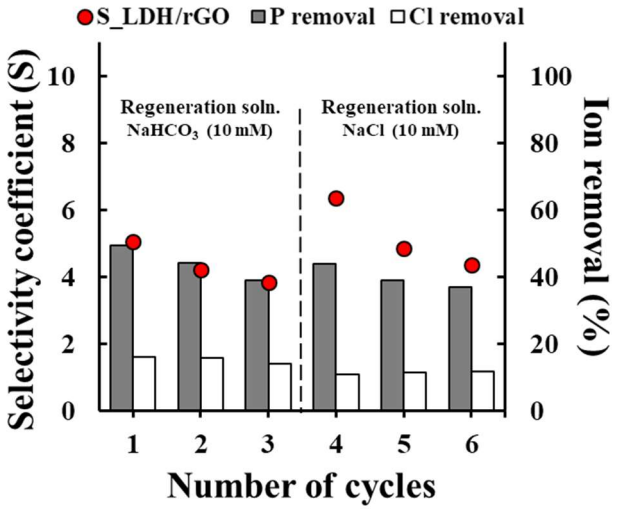

Figure 22. The selective coefficient (*S*) of LDH/rGO-PB system in different regeneration solutions (sodium bicarbonate and sodium chloride). For all capturing steps fom 1st cycle to 6th cycle, the mixed solution of 1 mM phosphate and 10 mM of chloride was used. The releasing step was conducted in sodium bicarbonate (10 mM, pH 8.5, from 1st cycle to 3th cycle), and sodium chloride (10 mM, pH 7.2, from 4th cycle to 6th cycle).

Table 2. Anion Composition of Han River Water (Korea)

Anions (pH 8.1)	Concentration [mg·L^{-1}, (mM)]	Concentration Ratio [mole of anions/mole of P·PO_4]
PO_4^{3-}(added)	0.38 (0.012)	1
Cl^-	32 (0.91)	76
NO_3^-	15.5 (0.25)	21
SO_4^{2-}	18.9 (0.20)	17

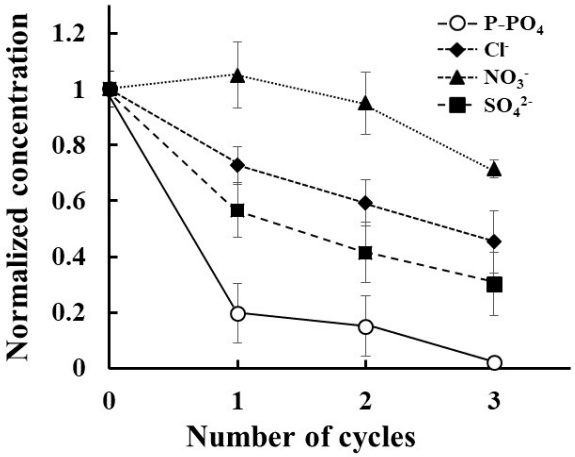

Figure 23. Phosphate removal from the real simulated water matrix (Han River, Seoul, Korea) via LDH/rGO-PB system. 0.4 mg·L-1 of phosphate was added in the real water matrix. In the releasing step, 10 mM of sodium hydroxide solution was used.

3.4. Summary

In this study, the phosphate selective removal of LDH/rGO-PB system was successfully demonstrated. With repeated capturing and release, the selective removal performance of LDH/rGO-PB system was sustained even when the chloride concentration was increased to 20 times higher than phosphate concentration. This phosphate selective performance of the LDH/rGO-PB system was also demonstrated by its high *S* value compared to conventional CDI consisted of activated carbon electrodes (6.1 for LDH/rGO, and 2.0 for activated carbon electrode). In addition, the LDH/rGO-PB system exhibited good energy efficiency and reusability. Furthermore, phosphate in the real water matrix (Han River, Seoul, Korea) was selectively removed. This result is explained by the high electrochemical selectivity of the LDH/rGO electrode for phosphate.

4. Enhanced Phosphate Removal Performance of Electrochemical Process

4.1. Introduction

CDI, which is electrochemical process for ion separation from water, has been regarded as alternative technology for water treatment due to its environmental benign characteristics, high energy efficiency, and simple operation. In general, CDI is composed of a pair of electrode, and the separator providing prevention of short circuit and water flow channel. With sequential charging/discharging steps, ions in aqueous media is electrochemically ad/desorbed via capacity of electrodes. For the conventional CDI, nanoporous activated carbon electrodes are used to separate ions by storing ions in EDL.

In the EDL storage of CDI, the interaction between ions and electrodes is simple electrostatic attraction (physisorption), which is non-specific. For this reason, CDI has difficulties to be applied further for other water treatment beyond desalination. When CDI was applied specific anion removal, conventional CDI showed a limitation with decreasing salt adsorption capacity of target anions as increasing competing anions concentration

(Huang, He et al. 2017). Therefore, for the practical application of CDI, selective phosphate removal is important issue because phosphate exists with higher concentration of other anions in water.

LDHs were used as a based material for phosphate selective electrode in CDI due to its affinity toward phosphate. With improved electrical conductivity, ZnAl-LDH and reduced graphene oxide composite (LDH/rGO) electrode showed selective behavior for phosphate in the CDI process consisted of LDH/rGO and PB (LDH/rGO-PB system). Phosphate was captured by ligand exchange reaction and intercalation with LDH part of LDH/rGO, which was facilitated by electrical driven oxidation of metal cations. The phosphate removal efficiency was almost maintained even when the molar ratio of phosphate to chloride was increasing from 1:5 to 1:20. Additionally, this LDH/rGO-PB system exhibited selective phosphate removal successfully in the real water matrix which has 77 times higher concentration of chloride compared to added phosphate (Han River, Seoul, Korea). However, for practical applications, the capacity of LDH/rGO electrode need to be improved with selective property toward phosphate. This can be achieved by thermal treatment leading the elimination of intrinsic intercalated anions that occupy active sites of LDHs.

In this study, the novel CDI process was examined for selective removal of phosphate, which was composed of thermal treated LDH/rGO electrode for capturing phosphate and an activated carbon electrode with a cation exchange membrane for capturing cations (tLDH/rGO-AC system). During charging step, CDI performance for phosphate removal was examined in aspect of capacity and selectivity according to different temperature for thermal treatment. In a discharging step, phosphate enrichment was attempted by collecting phosphate released from the electrode in a 20 ml of electrolyte. By achieving phosphate removal and enrichment processes, the LDH/rGO-AC system showed great potential as an alternative technology for phosphate removal/recovery.

4.2. Experimental Section

4.2.1. Preparation of Thermal Treated LDH/rGO Electrode

Prior to synthesis of LDH/rGO powder, rGO was prepared by reducing 2.5 $g \cdot L^{-1}$ of GO in 30 $g \cdot L^{-1}$ of L-ascorbic acid at 90℃ overnight (total volume is 50 ml). Then, obtained rGO was dispersed in 250 ml of solution containing 0.744, 0.479, and 0.526 g of $Zn(NO_3)_2 \cdot 6H_2O$, $Al(NO_3)_3 \cdot 9H_2O$ and urea, respectively. The LDH/rGO powder was synthesized after hydrothermal

process of this rGO dispersed solution at 95℃ for 24 h. Then, obtained LDH/rGO powder was well washed in deionized water and dried by using freeze drier (FDU-1200, Tokyo Rikakikai Co., LTd., Tokyo, Japan). The dried LDH/rGO powder was thermally treated with various temperature under N_2 atmosphere during 2 h with 5℃·min^{-1} of heating rate.

In order to fabricate freestanding electrode, thermal treated LDH/rGO (tLDH/rGO) powder was mixed with conducting agent and polytetrafluoroethylene (PTFE) as weight ratios of 8:1:1. Then, tLDH/rGO electrode was fabricated by the role-pressing method and dried in a vacuum oven. LDH/rGO electrode, without thermal treatment, was prepared with the same procedure. tLDH/rGO powder was analyzed by X-ray diffractometer (XRD, the Rigaku D-MAX2500, Tokyo, Japan) at 2 degree·min^{-1} to investigate the influence of thermal treatment on LDH structure. tLDH/rGO treated at 500℃ was used as a representative electrode when compared to pristine LDH/rGO electrode in the electrochemical system

4.2.2. Evaluation of tLDH/rGO-AC for phosphate removal

The semi-batch electrochemical system was prepared with the tLDH/rGO as a phosphate capturing electrode, and activated carbon electrode with a

cation exchange membrane as cation capturing electrode. tLDH/rGO treated at 500℃ was selected as an electrode of this system. Phosphate removal was conducted for 1 mM of phosphate solution at neutral pH which was prepared by adding two salts, sodium phosphate monobasic (NaH_2PO_4) and sodium phosphate dibasic (Na_2HPO_4) as the mole ratio of 1:1. To evaluate phosphate adsorption capacity, the cell was operated at 1.2 V with collecting samples depending on time during 8 h. For the selectivity test, a mixed solution of nitrate, sulfate, phosphate, chloride (1 mM of each anion) was used as a feed solution at 150 $mA \cdot g^{-1}$ during 4 h. Anion concentration in collected samples were measured by ion chromatography (DX-120, DIONEX, CA, USA).

4.2.3. Electrochemical Characterization

tLDH/rGO electrode was investigated by electrochemical method compared with pristine LDH/rGO electrode. Galvanostatic charge/discharge measurement was performed at 150 $mA \cdot g^{-1}$ with the potential range of working electrode from -0.6 V to 0.8 V vs. Ag/AgCl reference electrode. The cycle test of tLDH/rGO was also conducted during 100 cycle at 150 $mA \cdot g^{-1}$ without a reference electrode in the potential range from -1.0 V to 1.0 V. For all electrochemical analysis, excess activated carbon electrode was used as counter electrode, and 1 M of sodium phosphate with neutral pH was used as

an electrolyte. With the same configuration of galvanostatic charge/discharge measurement, the capacity of tLDH/rGO-AC system was measured without a reference electrode in the cell voltage range from -0.6 V to 1.0 V in 1 M of phosphate solution at neutral pH.

4.2.4. Applications to Phosphate Enrichment Process

Considering releasing step, captured phosphate should be released into effluent of releasing step in tLDH/rGO-AC system indicating the generation of secondary pollutant. To prevent generating secondary pollutant, phosphate enrichment was examined in tLDH/rGO-AC system by sustained an electrolyte of releasing step for next releasing steps. The 20 ml of mixed solution containing 10 mM of sodium hydroxide and 10 mM of sodium chloride was used as an electrolyte in releasing step, while the 100 ml of feed solution containing 1 mM of phosphate at neutral pH was used for capturing step. During 4 times repetition of capturing-releasing steps, electrolytes for each step were not changed to collecting released phosphate in the electrolyte of releasing step. Capturing step was conducted with 1.2 cell voltage for 4 h and releasing step was conducted with -1.2 V for 2 h.

4.3. Results and Discussion

4.3.1. Characterization of tLDH/rGO

In Figure 24, the influence of thermal treatment on LDH structure was investigated by XRD analysis. As shown in Figure 24 (a), 003, and 006 peaks were disappeared from 350℃ indicating a destroyed layered structure of LDH part within LDH/rGO electrode. Based in TGA profile, intercalated species were degraded from 200℃ to 300℃, which was corresponding with XRD patterns. The 2D structure of LDHs were collapsed by thermal treatment because a degradation of intercalated anions and water molecules. Around 10 wt% of LDH/rGO powder was decreased near 500℃ due to degradation of rGO whereas there is no significant change at 500℃ under the N_2. Therefore, the rGO part of LDH/rGO has been less damaged during thermal treatment in N_2 atmosphere compared with O_2 atmosphere.

The electrochemical characterization of tLDG/rGO electrode was also analyzed compared with pristine LDH/rGO electrode (Figure 25). As shown in Figure 25 (a), tLDH/rGO electrode has higher capacity (40 $mAh \cdot g^{-1}$) than that of pristine LDH/rGO electrode (25 $mAh \cdot g^{-1}$). This improvement can be explained by increasing active sites of thermal treated LDH/rGO electrode. In detail, during thermal treatment, degradation of the intercalated anions

(nitrate in this study) and water molecules provides free active sites where can absorb phosphate. It caused superior discharging capacity of tLDH/rGO electrode during 200 cycles although it was decreased as the cycle repeated (Figure 25 (b)).

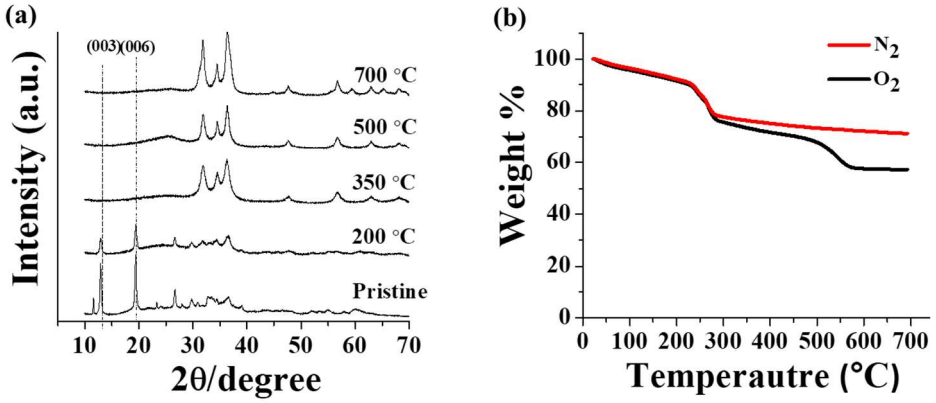

Figure 24. XRD patterns depending on thermal treatment temperature (a), and results of TGA (b) of LDH/rGO electrode.

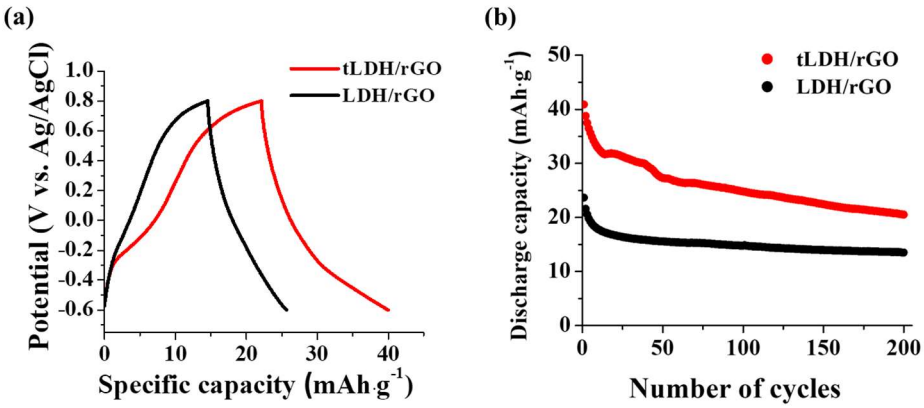

Figure 25. Galvanostatic charge/discharge curve (a), and discharging capacity profile in cyclability test (b) of tLDH/rGO electrode compared to pristine LDH/rGO electrode. During cyclability test, the cell potential range of one cycle was from -1 V to +1 V without a reference electrode. For both, 1 M of sodium phosphate with neutral pH was used, and current density was 150 $mA \cdot g^{-1}$.

4.3.2. Phosphate Removal Performance of tLDH/rGO-AC System

As shown in Figure 26 (a), phosphate removal of tLDH/rGO-AC system was examined for 1 mM of sodium phosphate solution with applying 1.2 V of cell voltage during 2 h compared to LDH/rGO-AC system with an identical condition. The capacity of tLDH/rGO electrode was 0.9 $mmol \cdot g^{-1}$ which was 2 times higher than 0.4 $mmol \cdot g^{-1}$ of LDH/rGO electrode. It is attributed to increased active sites of LDH part resulting from elimination of intercalated anions and water molecules after thermal treatment. This explanation was supported by XRD patterns of tLDH/rGO in Figure 24. As shown in Figure 26 (b), the appearance of new peaks near 20° in XRD pattern of used tLDH/rGO electrode refers to reconstruction of the collapsed structure of LDH part suggesting intercalation of phosphate.

The selective removal performance of tLDH/rGO-AC system and LDH/rGO-AC system was displayed in Figure 27 (a) and (b). As shown in Figure 27 (a), the concentration of phosphate was decreased from 1 mM to 6 mM during 4 h while the concentration changes of other anions were negligible. It is indicating a great selective performance of tLDH/rGO-AC system. This selective behavior was also observed in LDH/rGO-AC system (Figure 27 (b)), implying that selective property of tLDH/rGO electrode was

maintained after collapsing stacked structure of LDH part by thermal treatment.

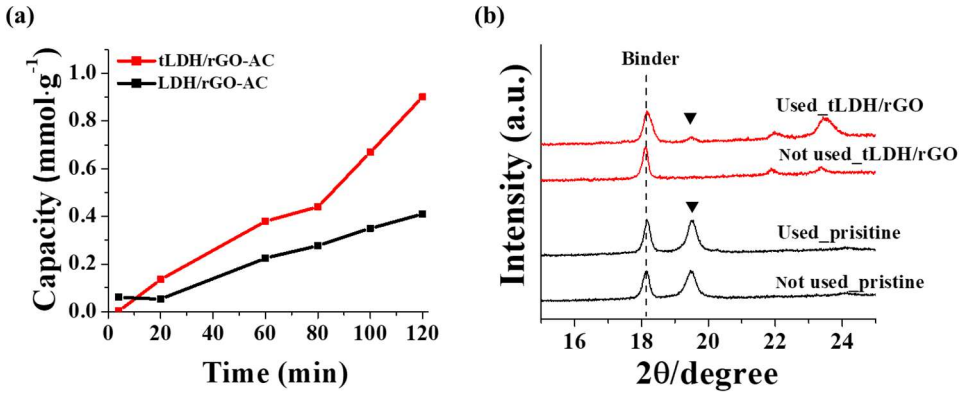

Figure 26. The comparison of capacity for phosphate removal between tLDH/rGO-AC system and LDH/rGO-AC system (a), and XRD patterns of used tLDH/rGO and LDH/rGO electrodes with not used electrodes (b). The comparison of capacity was conducted with applied 1.2 V of cell voltage during 2 h in 1mM of sodium phosphate at neutral pH. Note that tLDH/rGO and LDH/rGO electrodes were used in 1 mM of phosphate solution at neutral pH.

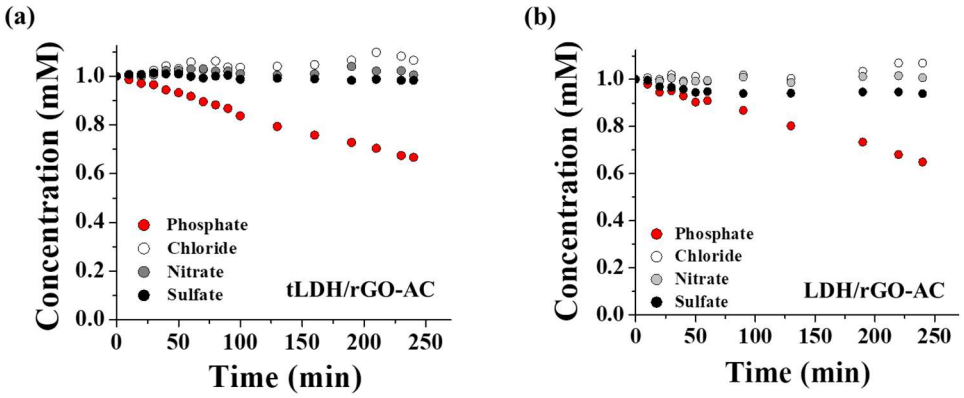

Figure 27. Phosphate removal in mixed solution of tLDH/rGO-AC system (a) and tLDH/rGO-AC system (b). Systems were operated at 150mA·g^{-1} of current density during 4 h in the mixture of phosphate, chloride, nitrate, and sulfate (1 mM of each anions) with sodium cation.

4.3.3. Phosphate Enrichment of tLDH/rGO-AC System

The electrochemical process for phosphate removal consisted of two steps, capturing step (charging process) for ion separation with, and releasing step (discharging process) for electrode regeneration by ion releasing from electrodes. Please note that discharged phosphate during releasing step should be considered in the phosphate treatment process. In this study, discharged phosphate of tLDH/rGO-AC system was collected for phosphate recovery as struvite, one of major form in phosphate recovery as a resource. In general, phosphate can be precipitated as struvite in a higher concentration of phosphate compared to feed solution of wastewater plant (below 10 $mg \cdot g^{-1}$). As shown in Figure 28, phosphate concentration of feed solution was decreased from 1.0 mM to 0.35 mM after successive four capturing-releasing process, while phosphate concentration was increased up to 1.7 mM. This result means that releasing step can be applied as enrichment process for phosphate recovery as struvite although only 50% of removed phosphate was collected in collecting solution.

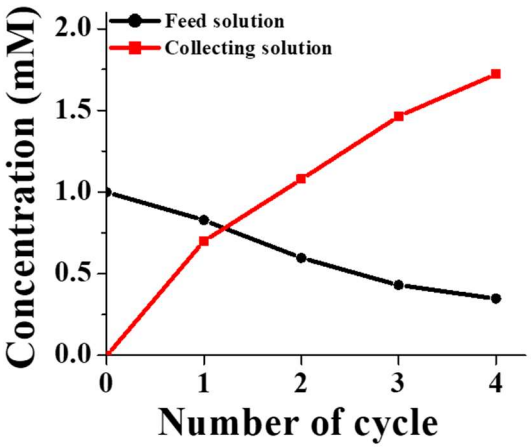

Figure 28. The result of phosphate enrichment in tLDH/rGO-AC system. For capturing process, 100 ml of sodium phosphate (1 mM) at neutral pH was used as a feed solution. For releasing process, 20 ml of sodium hydroxide and sodium chloride mixed solution (10 mM of each) was used as a phosphate collecting solution. Capturing step was conducted at constant voltage, 1.2 V for 4 hours, and releasing step was conducted at -1.2 V for 2 h.

4.4. Summary

In this study, the phosphate removal performance of tLDH/rGO-AC system was evaluated. tLDH/rGO-AC system showed two times higher capacity for phosphate removal compared to LDH/rGO-AC system with clear selective behavior. This enhancement can be explained by increasing active sites of tLDH/rGO occupied intercalated anions and water molecules after thermal treatment. With the result of phosphate enrichment during releasing step, the tLDH/rGO-AC system exhibited a great potential as phosphate removal/recovery process without generating secondary pollution.

5. Conclusion

In this dissertation, a novel electrochemical system of selective removal for phosphate was investigated. LDH/rGO electrode was applied as phosphate capturing electrode in this electrochemical system.

First of all, the concept of electrochemical system was successfully demonstrated by achieving selective removal for phosphate. LDH/rGO electrode was utilized in this system with PB electrode and cation exchange membrane for capturing cation. This LDH/rGO-PB system was operated by two steps, capturing/releasing steps, which are phosphate removal and electrode regeneration steps, respectively. During capturing step, the potential of LDH/rGO was increased with capturing phosphate from feed solution while the potential of PB was maintained at 0.2 V with intercalation of sodium cation. During releasing step, the potential of LDH/rGO was decreased with releasing phosphate into 10 mM of sodium hydroxide electrolyte while the potential of PB was conversed around 0.6 V. Most of all, selective behavior was observed in the electrochemical system, LDH/rGO-PB system, allowing maintained phosphate removal efficiency even in 20 times higher concentration of chloride. This selective behavior was clearly shown when compared to activated carbon system. In addition, LDH/rGO-PB system

removed phosphate successfully in the real water matrix (Han River, Seoul, Korea). It is attributed to electrochemical reaction between phosphate and LDH/rGO electrode allowing ligand exchange reaction and intercalation.

Second, the strategy of thermal treatment to enhance the performance of LDH/rGO electrode was investigated. In this study, excess activated carbon electrode with cation exchange membrane was used as cation capturing part for the practical application. The capacity of LDH/rGO was improved by thermal treatment resulted from increased active sites of LDH part. During thermal treatment, stacked structure of LDH was collapsed indicating elimination of intercalated anions and water molecules from interlayers that occupied the active sites. The capacity was increased from 25 $mAh \cdot g^{-1}$ to 40 $mAh \cdot g^{-1}$ after thermal treatment at 500°C. The phosphate removal capacity of tLDH/rGO-AC system was also two times higher than LDH/rGO-AC system for 1 mM of sodium phosphate solution. The selective removal of tLDH/rGO-AC system was also observed for 1 mM of phosphate in presence of nitrate, chloride, and sulfate as competing ions (1 mM of each anion). Furthermore, by using tLDH/rGO-AC system, phosphate enrichment was conducted by collecting released phosphate in releasing step with 50% of phosphate recovery. Therefore, tLDH/rGO-AC system could be effective process to

remove phosphate even in the presence of excess competing ions without generating secondary pollution.

References

Blair, J. W. and G. W. Murphy (1960). Electrochemical demineralization of water with porous electrodes of large surface area. University of Oklahoma: Norman, OK, ACS publications**:** 206-223.

Brousse, T., D. Bélanger and J. W. Long (2015). "To Be or Not To Be Pseudocapacitive?" Journal of The Electrochemical Society **162**(5): A5185-A5189.

Cao, Y., Q. Guo, Z. Shu, Y. Zhuang, Z. Yu, W. Guo, C. Zhang, M. Zhu, Q. Zhao and T. Ren (2016). "Application of calcined iowaite in arsenic removal from aqueous solution." Applied Clay Science **126**: 313-321.

Chen, Z., H. Zhang, C. Wu, Y. Wang and W. Li (2015). "A study of electrosorption selectivity of anions by activated carbon electrodes in capacitive deionization." Desalination **369**: 46-50.

Cheng, X., X. Huang, X. Wang, B. Zhao, A. Chen and D. Sun (2009). "Phosphate adsorption from sewage sludge filtrate using zinc-aluminum

layered double hydroxides." Journal of Hazardous Materials **169**(1-3): 958-964.

Chitrakar, R., S. Tezuka, A. Sonoda, K. Sakane, K. Ooi and T. Hirotsu (2005). "Adsorption of phosphate from seawater on calcined MgMn-layered double hydroxides." Journal of Colloid and Interface Science **290**(1): 45-51.

Cho, S., J.-W. Jang, K.-j. Kong, E. S. Kim, K.-H. Lee and J. S. Lee (2013). "Anion-Doped Mixed Metal Oxide Nanostructures Derived from Layered Double Hydroxide as Visible Light Photocatalysts." Advanced Functional Materials **23**(19): 2348-2356.

Cordell, D., J.-O. Drangert and S. White (2009). "The story of phosphorus: Global food security and food for thought." Global Environmental Change **19**(2): 292-305.

Farmer, J. C., D. V. Fix, G. V. Mack, R. W. Pekala and J. F. Poco (1995). Capacitive, deionization with carbon aerogel electrodes: carbonate, sulfate, and phosphate, Lawrence Livermore National Lab.

Fytianos, K., E. Voudrias and N. Raikos (1998). "Modelling of phosphorus removal from aqueous and wastewater samples using ferric iron." Environmental Pollution **101**(1): 123-130.

Gao, Z., J. Wang, Z. Li, W. Yang, B. Wang, M. Hou, Y. He, Q. Liu, T. Mann and P. Yang (2011). "Graphene nanosheet/Ni2+/Al3+ layered double-hydroxide composite as a novel electrode for a supercapacitor." Chemistry of Materials **23**(15): 3509-3516.

Ge, Z., X. Chen, X. Huang and Z. J. Ren (2018). "Capacitive deionization for nutrient recovery from wastewater with disinfection capability." Environmental Science: Water Research and Technology **4**(1): 33-39.

Goh, K. H., T. T. Lim and Z. Dong (2008). "Application of layered double hydroxides for removal of oxyanions: a review." Water Research **42**(6-7): 1343-1368.

Gu, Y., D. Xie, Y. Ma, W. Qin, H. Zhang, G. Wang, Y. Zhang and H. Zhao (2017). "Size Modulation of Zirconium-Based Metal Organic Frameworks for Highly Efficient Phosphate Remediation." ACS Applied Materials & Interfaces **9**(37): 32151-32160.

Gunther, F. (2005). "A solution to the heap problem: the doubly balanced agriculture: integration with population." Online: http://www. holon. se/folke/kurs/Distans/Ekofys/Recirk/Eng/balanced. shtml (zuletzt aufgerufen: 2013-09-20).

Hatami, H., A. Fotovat and A. Halajnia (2018). "Comparison of adsorption and desorption of phosphate on synthesized Zn-Al LDH by two methods in a simulated soil solution." Applied Clay Science **152**: 333-341.

Hou, C. H., P. Taboada-Serrano, S. Yiacoumi and C. Tsouris (2008). "Electrosorption selectivity of ions from mixtures of electrolytes inside nanopores." Journal of Chemical Physics **129**(22): 224703.

Huang, X., D. He, W. Tang, P. Kovalsky and T. D. Waite (2017). "Investigation of pH-dependent phosphate removal from wastewaters by membrane capacitive deionization (MCDI)." Environmental Science: Water Research & Technology **3**(5): 875-882.

Hummers Jr, W. S. and R. E. Offeman (1958). "Preparation of graphitic oxide." Journal of the American Chemical Society **80**(6): 1339-1339.

İrdemez, Ş., Y. Ş. Yildiz and V. Tosunoğlu (2006). "Optimization of phosphate removal from wastewater by electrocoagulation with aluminum plate electrodes." Separation and Purification Technology **52**(2): 394-401.

Islam, M. and R. Patel (2010). "Synthesis and physicochemical characterization of Zn/Al chloride layered double hydroxide and evaluation of its nitrate removal efficiency." Desalination **256**(1-3): 120-128.

Jin, Q., S. Zhang, T. Wen, J. Wang, P. Gu, G. Zhao, X. Wang, Z. Chen, T. Hayat and X. Wang (2018). "Simultaneous adsorption and oxidative degradation of Bisphenol A by zero-valent iron/iron carbide nanoparticles encapsulated in N-doped carbon matrix." Environmental Pollution **243**(Pt A): 218-227.

Khaldi, M., M. Badreddine, A. Legrouri, M. Chaouch, A. Barroug, A. De Roy and J. P. Besse (1998). "Preparation of a well-ordered layered nanocomposite from zinc–aluminum–chloride layered double hydroxide and hydrogenophosphate by ion exchange." Materials Research Bulletin **33**(12): 1835-1843.

Kim, H., J. Hong, Y.-U. Park, J. Kim, I. Hwang and K. Kang (2015). "Sodium Storage Behavior in Natural Graphite using Ether-based Electrolyte Systems." Advanced Functional Materials **25**(4): 534-541.

Kim, S., J. Lee, J. S. Kang, K. Jo, S. Kim, Y. E. Sung and J. Yoon (2015). "Lithium recovery from brine using a lambda-MnO2/activated carbon hybrid supercapacitor system." Chemosphere **125**: 50-56.

Kim, S., J. Lee, C. Kim and J. Yoon (2016). "Na2FeP2O7 as a Novel Material for Hybrid Capacitive Deionization." Electrochimica Acta **203**: 265-271.

Kim, S., H. Yoon, D. Shin, J. Lee and J. Yoon (2017). "Electrochemical selective ion separation in capacitive deionization with sodium

manganese oxide." Journal of Colloid and Interface Science **506**: 644-648.

Kuzawa, K., Y. J. Jung, Y. Kiso, T. Yamada, M. Nagai and T. G. Lee (2006). "Phosphate removal and recovery with a synthetic hydrotalcite as an adsorbent." Chemosphere **62**(1): 45-52.

Lai, Y.-T., W.-T. Liu, L.-J. Chen, M.-C. Chang, C.-Y. Lee and N.-H. Tai (2019). "Electro-assisted selective uptake/release of phosphate using a graphene oxide/MgMn-layered double hydroxide composite." Journal of Materials Chemistry A **7**(8): 3962-3970.

Lee, J., S. Kim, C. Kim and J. Yoon (2014). "Hybrid capacitive deionization to enhance the desalination performance of capacitive techniques." Energy & Environmental Science **7**(11): 3683-3689.

Lee, J., S. Kim and J. Yoon (2017). "Rocking Chair Desalination Battery Based on Prussian Blue Electrodes." ACS Omega **2**(4): 1653-1659.

Long, J., Z. Yang, J. Huang and X. Zeng (2017). "Self-assembly of exfoliated layered double hydroxide and graphene nanosheets for electrochemical energy storage in zinc/nickel secondary batteries." Journal of Power Sources **359**: 111-118.

Macías, C., P. Lavela, G. Rasines, M. C. Zafra, J. L. Tirado and C. O. Ania (2014). "Improved electro-assisted removal of phosphates and nitrates

using mesoporous carbon aerogels with controlled porosity." Journal of Applied Electrochemistry **44**(8): 963-976.

Mayer, B. K., L. A. Baker, T. H. Boyer, P. Drechsel, M. Gifford, M. A. Hanjra, P. Parameswaran, J. Stoltzfus, P. Westerhoff and B. E. Rittmann (2016). "Total Value of Phosphorus Recovery." Environmental Science & Technology **50**(13): 6606-6620.

Morel, F., J. G. Hering and J. G. Hering (1993). Principles and Applications of Aquatic Chemistry, John Wiley & Sons.

Morimoto, K., S. Anraku, J. Hoshino, T. Yoneda and T. Sato (2012). "Surface complexation reactions of inorganic anions on hydrotalcite-like compounds." Journal of Colloid and Interface Science **384**(1): 99-104.

Neufeld, R. D. and G. Thodos (1969). "Removal of orthophosphates from aqueous solutions with activated alumina." Environmental Science & Technology **3**(7): 661-667.

Parida, K. M., M. Sahoo and S. Singha (2010). "Synthesis and characterization of a Fe(III)-Schiff base complex in a Zn-Al LDH host for cyclohexane oxidation." Journal of Molecular Catalysis A: Chemical **329**(1-2): 7-12.

Pastushok, O., F. Zhao, D. L. Ramasamy and M. Sillanpää (2019). "Nitrate removal and recovery by capacitive deionization (CDI)." Chemical Engineering Journal **375**.

Pretty, J. N., C. F. Mason, D. B. Nedwell, R. E. Hine, S. Leaf and R. Dils (2003). Environmental costs of freshwater eutrophication in England and Wales, ACS Publications.

Rittmann, B. E., B. Mayer, P. Westerhoff and M. Edwards (2011). "Capturing the lost phosphorus." Chemosphere **84**(6): 846-853.

Seftel, E. M., E. Popovici, M. Mertens, K. D. Witte, G. V. Tendeloo, P. Cool and E. F. Vansant (2008). "Zn–Al layered double hydroxides: Synthesis, characterization and photocatalytic application." Microporous and Mesoporous Materials **113**(1-3): 296-304.

Shao, M., R. Zhang, Z. Li, M. Wei, D. G. Evans and X. Duan (2015). "Layered double hydroxides toward electrochemical energy storage and conversion: design, synthesis and applications." Chemical Communications **51**(88): 15880-15893.

Smil, V. (2000). "Phosphorus in the environment: natural flows and human interferences." Annual review of energy and the environment **25**(1): 53-88.

Song, F. and X. Hu (2014). "Exfoliation of layered double hydroxides for enhanced oxygen evolution catalysis." Nature Communications **5**: 4477.

Steen, I. (1998). "Phosphorus availability in the 21st century: management of a non-renewable resource." Phosphorus Potassium **217**: 25-31.

Su, X., J. Hübner, M. J. Kauke, L. Dalbosco, J. Thomas, C. C. Gonzalez, E. Zhu, M. Franzreb, T. F. Jamison and T. A. Hatton (2017). "Redox Interfaces for Electrochemically Controlled Protein–Surface Interactions: Bioseparations and Heterogeneous Enzyme Catalysis." Chemistry of Materials **29**(13): 5702-5712.

Sun, J., Q. Yang, D. Wang, S. Wang, F. Chen, Y. Zhong, K. Yi, F. Yao, C. Jiang, S. Li, X. Li and G. Zeng (2017). "Nickel toxicity to the performance and microbial community of enhanced biological phosphorus removal system." Chemical Engineering Journal **313**: 415-423.

Sun, L., Y. Zhang, Y. Zhang, H. Si, W. Qin and Y. Zhang (2018). "Reduced graphene oxide nanosheet modified NiMn-LDH nanoflake arrays for high-performance supercapacitors." Chemical Communications **54**(72): 10172-10175.

Sun, Z., L. Chai, M. Liu, Y. Shu, Q. Li, Y. Wang and D. Qiu (2018). "Effect of the electronegativity on the electrosorption selectivity of anions during capacitive deionization." Chemosphere **195**: 282-290.

Tang, W., P. Kovalsky, D. He and T. D. Waite (2015). "Fluoride and nitrate removal from brackish groundwaters by batch-mode capacitive deionization." Water Research **84**: 342-349.

Tezuka, S., R. Chitrakar, K. Sakane, A. Sonoda, K. Ooi and T. Tomida (2004). "The Synthesis and Phosphate Adsorptive Properties of Mg(II)–Mn(III) Layered Double Hydroxides and Their Heat-Treated Materials." Bulletin of the Chemical Society of Japan **77**(11): 2101-2107.

Wang, J., T. Zhang, M. Li, Y. Yang, P. Lu, P. Ning and Q. Wang (2018). "Arsenic removal from water/wastewater using layered double hydroxide derived adsorbents, a critical review." RSC Advances **8**(40): 22694-22709.

Yang, K., L.-g. Yan, Y.-m. Yang, S.-j. Yu, R.-r. Shan, H.-q. Yu, B.-c. Zhu and B. Du (2014). "Adsorptive removal of phosphate by Mg–Al and Zn–Al layered double hydroxides: kinetics, isotherms and mechanisms." Separation and Purification Technology **124**: 36-42.

Yang, Q., X. Wang, W. Luo, J. Sun, Q. Xu, F. Chen, J. Zhao, S. Wang, F. Yao, D. Wang, X. Li and G. Zeng (2018). "Effectiveness and

mechanisms of phosphate adsorption on iron-modified biochars derived from waste activated sludge." Bioresource Technology **247**: 537-544.

Yang, Y., L. C. Kao, Y. Liu, K. Sun, H. Yu, J. Guo, S. Y. H. Liou and M. R. Hoffmann (2018). "Cobalt-Doped Black TiO2 Nanotube Array as a Stable Anode for Oxygen Evolution and Electrochemical Wastewater Treatment." ACS catalysis **8**(5): 4278-4287.

Yoon, H., J. Lee, S. Kim and J. Yoon (2018). "Electrochemical sodium ion impurity removal system for producing high purity KCl." Hydrometallurgy **175**: 354-358.

Yoon, H., J. Lee, S. Kim and J. Yoon (2019). "Review of concepts and applications of electrochemical ion separation (EIONS) process." Separation and Purification Technology **215**: 190-207.

Yu, L., N. Shi, Q. Liu, J. Wang, B. Yang, B. Wang, H. Yan, Y. Sun and X. Jing (2014). "Facile synthesis of exfoliated Co-Al LDH-carbon nanotube composites with high performance as supercapacitor electrodes." Physical Chemistry Chemical Physics **16**(33): 17936-17942.

Zafra, M. C., P. Lavela, C. Macías, G. Rasines and J. L. Tirado (2013). "Electrosorption of environmental concerning anions on a highly porous carbon aerogel." Journal of Electroanalytical Chemistry **708**: 80-86.

Zhang, K., Z. P. Xu, J. Lu, Z. Y. Tang, H. J. Zhao, D. A. Good and M. Q. Wei (2014). "Potential for layered double hydroxides-based, innovative drug delivery systems." International Journal of Molecular Sciences **15**(5): 7409-7428.

Zhu, E., X. Hong, Z. Ye, K. S. Hui and K. N. Hui (2019). "Influence of various experimental parameters on the capacitive removal of phosphate from aqueous solutions using LDHs/AC composite electrodes." Separation and Purification Technology.

국문초록

과량의 인산이온이 물 속에 존재하는 경우 심각한 녹조현상이 발생할 수 있기 때문에, 물속의 인산이온을 제거하는 것은 매우 중요한 문제이다. 인산 이온을 제거하기 위한 기존 기술로서 화학적 침전, 활성 슬러지법, 그리고 흡착 공정이 있다. 이러한 기존 기술들은 과량의 화학물질을 사용해야 하고, 슬러지를 발생시키기 때문에 2 차 오염을 야기한다는 한계점이 있다. 그렇기 때문에, 친환경적이며 에너지 효율성이 높고, 간단한 운전을 장점으로 갖는 전기화학적 이온제거 공정인 축전식 탈염공정 (Capacitive deionization, CDI)이 대체 기술로서 고려되고 있다. 그러나 기존의 CDI 는 양극의 활성탄 표면에 음이온을 붙이는 현상을 사용하기 때문에, 인산 이온에 대한 선택성이 부족하다는 단점을 지니고 있다. 실재 공정에서 인산 이온은 대부분 보다 높은 농도의 경쟁 이온들과 존재하게 된다는 점을 보았을 때, 선택성의 문제는 매우 중요하다고 할 수 있다.

본 학위 논문에서는, CDI 에서의 인산 선택적 제거를 달성하고 인산 선택적 흡착물질을 전극으로 활용한 새로운 CDI 시스템을

제안하였다. 이중층 수산화물과 환원된 산화 그래핀의 복합 재료 LDH/rGO 를 인산 선택적 전극으로 활용하고, 양이온을 제거하기 위해서 nickel hexacyanoferrate 프러시안 블루 전극과 양이온 교환막을 사용하여 LDH/rGO-PB 시스템을 구성하였다. LDH/rGO-PB 시스템은 염소 이온의 농도가 인산 이온의 농도보다 20 배 높음에도 불구하고, 인산 이온에 대한 제거 성능이 유지되는 거동을 보이며 인산 선택적 제거 성능을 보였다. 이는 주로 커패시티브한 거동에 의해 촉진된 인산이온과 LDH/rGO 전극 간의 리간드 교환 반응과 이온교환을 통한 삽입 반응으로 설명 할 수 있다. 이 시스템의 인산 선택적 제거 거동은 실제 한강물을 대상으로도 확인 할 수 있었다.

다음으로, 열처리를 통한 LDH/rGO 전극의 인산 이온 제거 성능 향상에 대해 연구하였다. 500℃에서 열처리 된 전극인 tLDH/rGO 와 함께, 양이온 교환막과 과량의 활성탄 전극을 사용해 tLDH/rGO−AC 시스템을 구성하였다. tLDH/rGO−AC 시스템은 중성의 1 mM 인산 이온을 대상으로, 약 0.9 $mmol \cdot g^{-1}$ 의 인산 이온 제거 용량을 보였으며, 이는

LDH/rGO-AC 시스템의 약 두 배에 달하는 용량이다. 이러한 성능의 증가는, tLDH/rGO 전극의 충방전 용량이 LDH/rGO 전극과 비교해서 약 60% 상승된 결과와 부합한다. 또한, 전극 재생공정에서 전극으로부터 떨어져 나오는 인산이온을 특정 전해 용액에 축적시키는 것으로 인산 이온 농축 실험을 수행하였다. 이 농축 공정은 인산 이온을 struvite 의 형태로 회수하기 위한 전처리 공정으로 활용 될 수 있다. 선택적 인산제거 능력과 인산 농축 공정으로 활용이 가능하다는 점에서, 본 시스템은 인산 이온 제거 및 회수를 위한 효과적인 전략으로 충분한 잠재력을 보여준다고 할 수 있다.

주요어: 전기화학적 수처리 시스템; 축전식 탈염 기술; 수산화 이중층 구조체; 환원된 산화 그래핀; 인산 이온 제거; 인산 회수

학번: 2015-30207